GEOMETRY AND CAPPING LAYER EFFECT ON COPPER LINES ELECTROMIGRATION TEST

A Thesis

by

MINGQIAN LI

Submitted to the Office of Graduate and Professional Studies of
Texas A&M University
in partial fulfillment of the requirements for the degree of

MASTER OF SCIENCE

Chair of Committee,	Yue Kuo
Co-Chair of Committee,	Philip Hemmer
Committee Members,	Gwan Choi
	Harlan Rusty Harris
Head of Department,	Miroslav Begovic

December 2019

Major Subject: Electrical Engineering

ABSTRACT

Copper (Cu) interconnect lines are widely used in advanced, high-density integrated circuits (ICs), large-area flat panel displays, and many nano and microelectronic and optoelectronic products. Compared with aluminum (Al), Cu has many advantages, such as the higher conductivity and longer lifetime. However, Cu is difficult to etch into fine lines using the conventional plasma etching method because the reaction product is nonvolatile. Another problem of Cu interconnect lines is that it has poor adhesion to the dielectric film unless an adhesion layer is used. Recently, Kuo's group solved the etching problem with a novel room-temperature process that consumes the Cu thin film with a plasma reaction and then removes the reaction product with a liquid solution. This method has been used in the fabrication of ICs and TFT LCDs.

One of the most critical issues in applying Cu lines in products is the reliability – electromigration (EM) lifetime prediction. As the IC keeps shrinking, the geometry effect on the lifetime of the thin Cu line is important especially for advanced products. Previously, Kuo's group had studied temperature and mechanical bending effects on the Cu fine line's lifetime. Geometry effects on the lifetime of the Al or Al-Cu alloy line have also been discussed before. However, there are few reports on the geometry effect on the Cu fine line prepared by the plasma-based etch process. In this research, the author investigated the relationship between the Cu line width or length and the EM failure time. The change of the line resistance with the stress time has also been studied.

The capping layer effect is very important in multi-layer devices. There were some research studies on Cu capping layer before, i.e., Ag layer to protect Cu oxidation and SiN layer as interlayer

dielectrics. However, few studies had been done on the TiW capping layer effect on plasma etched Cu lines. In this study, the TiW capping layer effect on lifetime has been studied.

ACKNOWLEDGEMENTS

I would like to thank all the people that helped me to finish this thesis. First of all, I really appreciate Dr. Yue Kuo's support, not only financially, but also academically. The suggestions and advice he gave me are very valuable and will never be obsolete. His encouragement provides me confidence to finish my master study. I learned a lot these years under his instruction.

Thanks also go to my friends and former colleagues, S. Zhang, X. Jiang and G. Liu. Jiang and Zhang taught me how to use and maintain the complicated machines. Without their help, my research progress would be much slower. The electromigration test program was written by Liu. The program is powerful and very useful for my work. I also appreciate J. Su for helping me make samples and doing some temperature calculation.

Finally, thanks to my parents for their encouragement. They taught me how to be a good person. They could use the money they saved to have a better life, but instead they paid the tuition for me and let me to pursue the life I want.

CONTRIBUTORS AND FUNDING SOURCES

Contributors

This work was supported by a thesis committee consisting of Professor Yue Kuo, Philip Hemmer, Harlan Harris and Gwan Choi of the Department of electrical engineering.

The electromigration test program used in this research was written by previous group student Guojun Liu.

All other work conducted for the thesis was completed by the student independently.

Funding Sources

This research is supported by National Science Foundation CMMI program project #1633580.

TABLE OF CONTENTS

LIST OF FIGURES

LIST OF TABLES

1. INTRODUCTION

1.1 Research background

In advanced, high-density ICs and microelectronic products, Copper (Cu) interconnect lines are widely used. Compared with aluminum (Al), Cu has many advantages, such as the lower resistivity and longer lifetime. However, Cu is difficult to etch into fine lines using the conventional plasma etching method because the reaction product is nonvolatile. Another problem of Cu interconnect is that it has poor adhesion to the dielectric film unless an adhesion layer is used. Kuo's group first reported a solution for the etch problem with a novel room-temperature process that consumed the exposed Cu thin film with a plasma reaction followed by the stripping of the reaction product with a HCl solution [1-3]. This method has been used in the fabrication of Ics and TFT LCDs [4].

One of the most critical issues in applying Cu lines in products is the reliability – electromigration (EM) lifetime prediction [5]. As the IC keeps shrinking, the geometry effect on the lifetime of the thin Cu line is important especially for advanced products. Previously, the Kuo's group had studied temperature and mechanical bending effects on the Cu fine line's lifetime [6-7]. Geometry effects on the lifetime of the Al or Al- Cu alloy line have also been discussed before [8-9]. However, there are few reports on the geometry effect on the Cu fine line prepared by the plasma-based etch process [10-11]. In this research, author investigated the relationship between the Cu line width or length and the EM failure time. The change of the line resistance with the stress time has also been studied.

Cu with barrier layer, i.e., TiW/Cu was deposited on the Corning glass. Then, the TiW/Cu layer was etched into lines with different geometry size. After etching, lines with different width

were tested under the same current density, so that the line width effect can be observed. In this process, two kind of curves were recorded, i.e., resistance vs time and breakdown time vs current density. According to these two curves, a Cu EM break down model was established to explain the how EM happened and how did EM effect the lines lifetime.

There were some researches on Cu capping layer before, i.e., Ag layer to protect Cu oxidation and SiN layer as interlayer dielectrics [12-13]. However, there are few studies on TiW capping layer effect on Cu lines. In this study, the TiW capping layer effect on the lifetime is studied.

Two types of structures, i.e., TiW /Cu and TiW /Cu /TiW, were deposited on the Corning glass. Then both of two kinds of lines with same geometry character were tested under the same current density to observe the capping layer effect.

1.2 Traditional Cu etching method introduction

1.2.1 CMP Cu etching method

Chemical Mechanical Polishing (CMP) is one of the most common Cu etching methods, which is widely used in industry now. Figure 1.1 shows the structure of the Cu lines before and after CMP etching method.

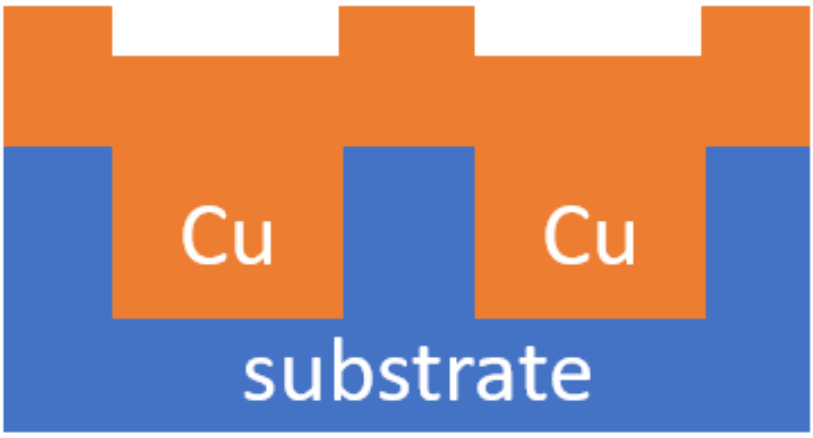

(a)

(b)

Figure 1.1 Sample structure before and after CMP etching. (a) before CMP etching process, (b) after CMP etching process.

Previous study [14] shows that Cu could be remove during CMP in Acidic H_2O_2 Slurry. The chemical reactions in this process could be summarized as follows [14].

$$2Cu + H_2O \rightarrow Cu_2O + 2H^+ + 2e^- \quad (1\text{-}1)$$

$$Cu_2O + H_2O \rightarrow 2CuO + 2H^+ + 2e^- \quad (1\text{-}2)$$

$$Cu_2O + 3H_2O \rightarrow 2Cu(OH)_2 + 2H^+ + 2e^- \quad (1\text{-}3)$$

The Cu rate with this CMP method is shown in Figure 1.2.

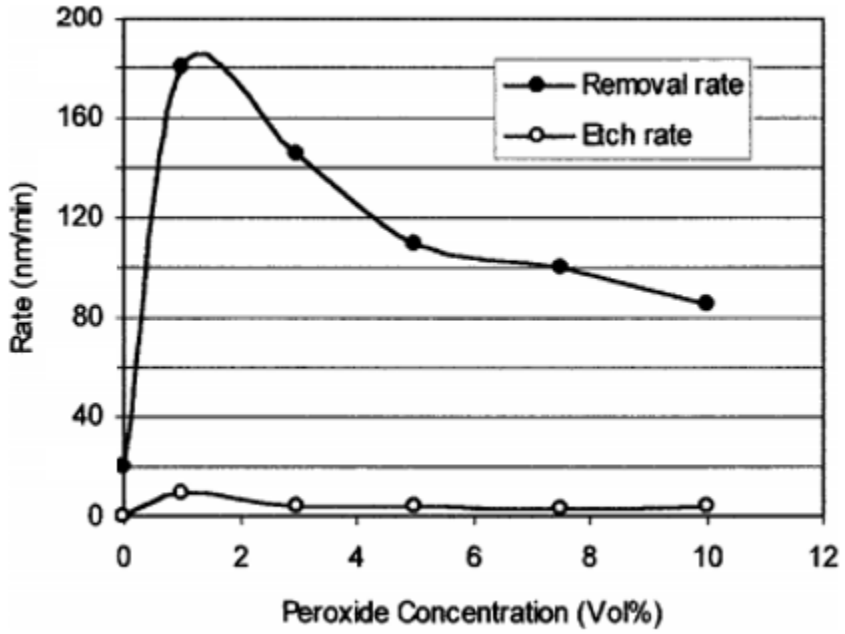

Figure 1.2 Cu removal and etch rate during CMP in Acidic H_2O_2 Slurry. Reprinted from ref. 14.

According to Figure 1.2, the maximum removal rate of this CMP method is about 190 nm per minutes, which is lower than the Cl_2 plasma etching process. Also, this 190 nm per minute removal rate can only be achieved at the 1% peroxide concentration. When the concentration is lower than 1%, the removal rate increased from 20 nm per minute to 190 nm per minute. As the concentration increases, the Cu removal rate decreases from 190 nm per minute to 90 nm per minute. The problem of this etching method is that the peroxide concentration has to been maintained at the concentration of 1%. During the process, the peroxide concentration decreases. As Figure 1.1 shows, if the concentration is not maintained, it will decrease because of the

chemical reaction and the etch rate will decrease drastically as well. Besides, if the peroxide concentration is higher than 1%, Cu layer will have the oxidation problem, which can reduce the Cu lines lifetime.

There are also some lacks for the traditional CMP method, such as stress cracking, delaminating at the layer's interfaces. And for the most used CMP in industry nowadays, oxide polishing process, has one defect. The blind polishing is hard to determine whether the required amount of material has been removed or not. Sometimes when the wafer is not flat or not uniformed, the wafer has to be remade and still has a higher chance to fail.

As Figure 1.1 shows, CMP can only make Cu lines which are inserted to the substrate. It cannot achieve the salient structure, which Cu lines are on the surface of the substrate, shown in Figure 1.3. The Cl_2/HCl plasma etching method, however, can achieve both mosaic and salient structure with the appropriate mask patterns.

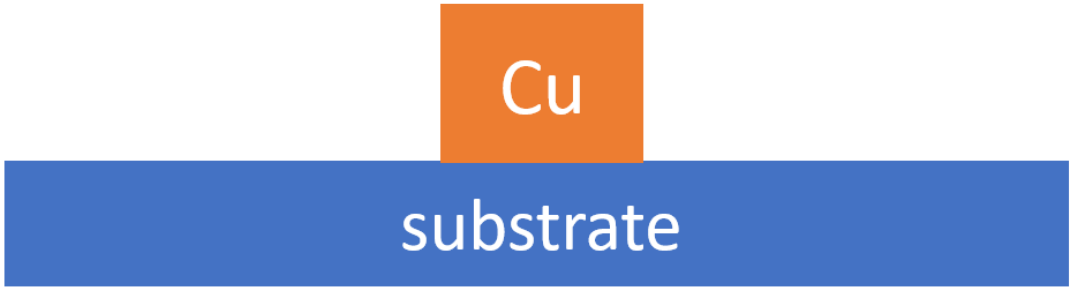

Figure 1.3 Cu lines with salient structure.

1.2.2 Cu wet etching with $FeCl_3$/$CuCl_2$ solution

There are also some Cu wet etching methods with $FeCl_3$ or $CuCl_2$ solution to achieve Cu lines with salient structure. These solution etching methods are leading technique for creating

circuit boards. Previous study [15] shows the wet etching method has higher etch rate than the plasma etching method. Figure 1.4 shows relationship between the etch rate and the concentration of enchant with different solution ($FeCl_3$ and $CuCl_2$).

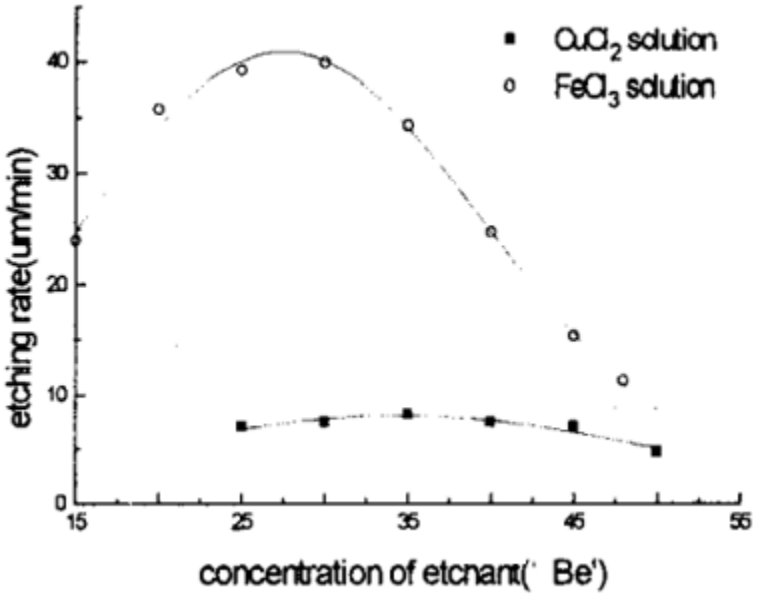

Figure 1.4 Relationship between concentration and Cu etching rate with different solution ($FeCl_3$ and $CuCl_2$). Adapted from ref. 15.

According to Figure 1.4, $FeCl_3$ solution has higher Cu etch rate than $CuCl_2$ solution under the same concentration. The reactions during the etching with $FeCl_3$ solution could be described as follows [15].

$$Cu + Fe^{3+} + 3Cl^- = CuCl_3^{2-} + Fe^{2+} \quad \text{(on etching surface)} \tag{1-4}$$

$$CuCl_3^{2-} + Fe^{3+} = Cu^{2+} + Fe^{2+} + 3Cl^- \quad \text{(in bulk solution)} \tag{1-5}$$

$$CuCl_3^{2-} = CuCl(\downarrow) + 2Cl^-$$
(on etching surface)

(1-6)

The chemical reaction of Cu etching is determined by diffusion of Fe^{3+}. The Fe^{3+} ions in the solution diffuse to Cu surface, because the Fe^{3+} ions concentration is low at the Cu surface due to Cu-Fe^{3+} reaction. However, the CuCl formation on Cu surface slows down the reaction, because CuCl film is passive for Fe^{3+} ions to penetrate. Figure 1.5 shows the etch rate change during the Cu etching process.

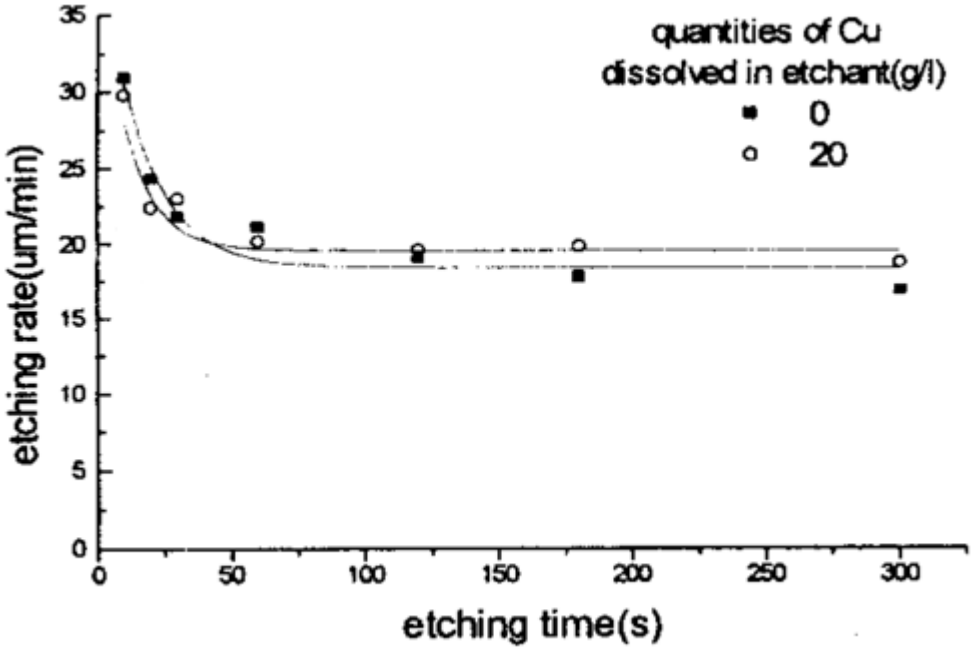

Figure 1.5 Cu etch rate during the Cu wet etching process. Reprinted from ref. 15.

According to Figure 1.5, the Cu etch rate decreases during the Cu etching process. In the first 60 s, the etch rate drops dramatically and starts to decrease slowly after one minute. The etch rate drop could explained by the CuCl formation on the Cu surface. At first, the etch rate is high

because there are plenty of $FeCl^{3+}$ on the Cu surface. As the reaction continuing, the concentration of Fe^{3+} ions start to decrease. CuCl also starts to form on the Cu surface to prevent the reaction between the Fe^{3+} and Cu. After one minute, the etch rate is determined by the time that Fe^{3+} ions need to travel through the CuCl passivation layer, not the Fe^{3+} ions concentration, so the decreasing speed of the etch starts to slow down. The inconsistent etch rate is hard to control, especially when it comes to nanoscale. A few seconds difference may cause undercut or incomplete etching problems. In the plasma etching process, when high energy is added, the ions can travel through the swell $CuCl_x$ and react with Cu atoms, so the etch rate of plasma etching method is more consistent than wet etching.

Another problem of the wet etching is that the etch rate is too high for some nanoscale structures. According to Figure 1.5, it only takes about 1 second to etch a Cu layer with thickness of 200 nm. In this case, when the samples are immersed into the solution, they need to be taken out immediately, otherwise the over etch would become a problem. This operation requires high time precision and it is hard to control when the Cu lines comes to nanometer scale.

A common drawback of wet etching method is the isotropic etching direction. The chemical reaction not only happens at the vertical direction, but also happens at the horizontal direction. The isotropic etching direction can cause serious undercut problem. The plasma etching, however, the undercut is not a very serious issue because most of the etching reaction happens at the vertical direction. Figure 1.6 shows the different cross section structure after wet etching and plasma etching. The actual proportion of each layer is different with the proportion shown in Figure 1.6. Figure 1.6 only shows the mechanism.

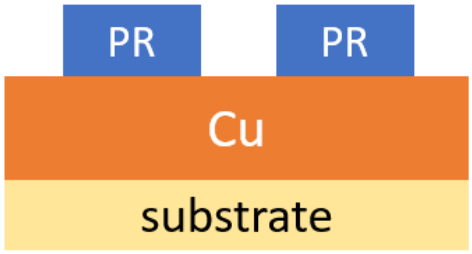

(a)

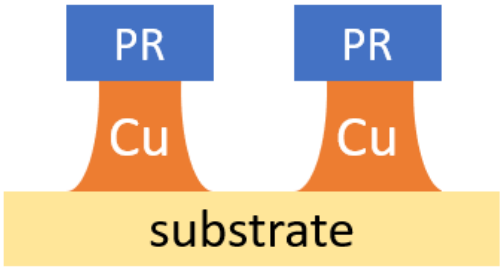

(b)

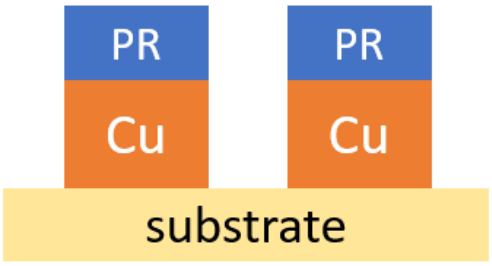

(c)

Figure 1.6 Structure difference between wet etching and plasma etching. (a) original structure, (b) after wet etching, (c) after plasma etching.

1.3 Cl_2/HCl plasma-based Cu etching

1.3.1 Cl_2/HCl plasma-based etching with HCl dipping

The Cl_2/HCl plasma etching method is first discovered by Dr. Kuo's group in 1999 [16]. This etching procedure can be summarized Figure 1.7.

Figure 1.7 Cu plasma etching process. Adapted from ref. 16.

The Cu compound in Figure 1.7 is $CuCl_x$, which is consisted of $CuCl_2$ and CuCl. The etching process pressure is usually from 10 mTorr to 100 mTorr at room temperature. At higher process temperature, the Cu etch rate is higher. After the Cu is exposed to the Cl_2/HCl plasma, Cu will be converted into $CuCl_x$. $CuCl_x$ has larger volume than Cu, resulting in the swelling effect. After conversion, the $CuCl_x$ part is even thicker than the photoresist layer. Figure 1.8 shows the mechanism of the conversion form Cu to $CuCl_x$.

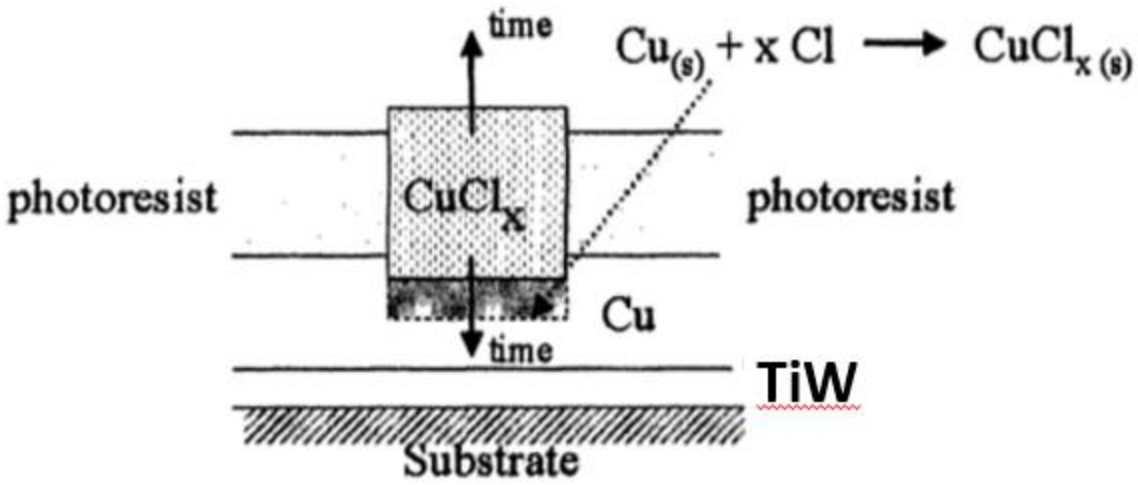

Figure 1.8 Simplified Cu swelling mechanism during the Cl_2/HCl plasma exposure. Adapted from ref. 16.

The main reaction shows in Figure 1.8 is between Cu and Cl. The Cl_2 flow rate is half as the HCl flow rate to achieve the same Cu etch rate. For example, if the Cu conversion rate is 100 nm per minute with 20 sccm HCl gas under the room temperature condition, it only needs 10 sccm Cl_2 to achieve the same Cu etch rate under the same condition [17].

The volume of the $CuCl_x$ is about 6 times larger than the original Cu. Figure 1.8 shows the Cu swelling effect after exposed to the Cl_2/HCl plasma.

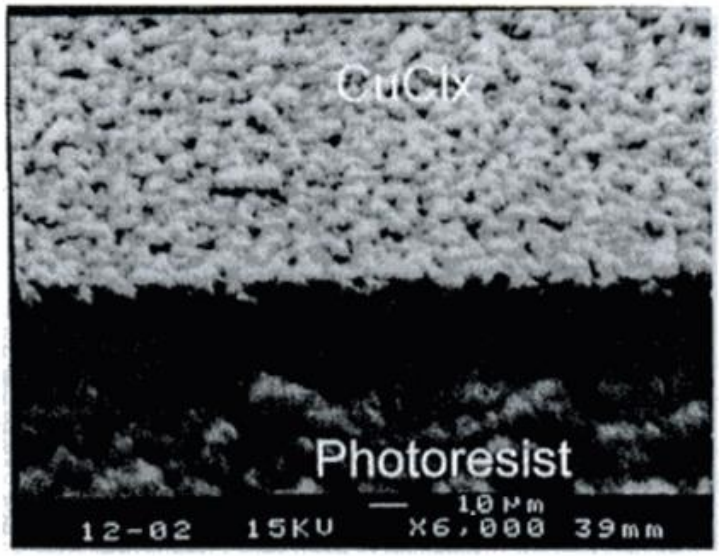

(a)

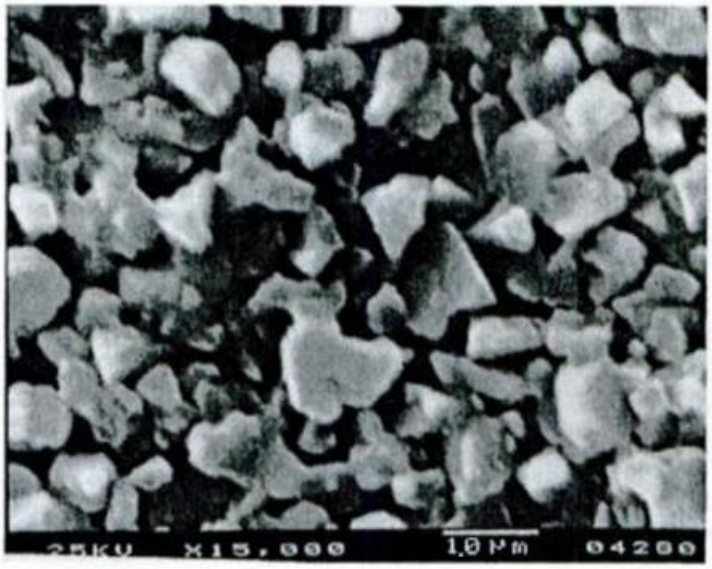

(b)

Figure 1.9 $CuCl_x$ SEM images from different views. (a) side view of Cu and photoresist surface after exposed to Cl_2/HCl plasma, (b) top view of $CuCl_x$ compound. Adapted from ref. 16.

Figure 1.9 (a) shows that the $CuCl_x$ rough and granular surface from the side view. Figure 1.9 (b) shows the columnar structure of the surface $CuCl_x$ from top view. The rough and granular surface of the $CuCl_x$ surface may be caused by the uneven plasma reaction on the Cu surface.

The columnar structure can increase the anisotropic etching rate on the vertical direction. The $CuCl_x$ columnar structure is due to the grain boundaries orientation in the original Cu layer. In the original Cu film, most of the grain boundaries are almost perpendicular to the substrate [16]. The vertical direction of the grain boundaries also causes the Cu chlorination reaction proceeds anisotropically from the surface toward the bulk of the film. The Cu conversion rate in the vertical direction is much faster than that in the horizontal direction. Most of other metals can form gas compound with Cl and can be removed from the chamber. CuCl, however, is very sticky compound. It accumulates on Cu surface. Once CuCl forms at the grain boundary area, ions bombardment can knock it down to the bottom, because the molecule support at the grain boundary area is weak. That's why when CuCl grows, the ions bombardment from the vertical direction can force the CuCl keeps the granular structure.

Figure 1.10 shows a vertical Cu profile after the removal of the CuClx reaction product and the photoresist. This kind of profile could be obtained under different etching conditions.

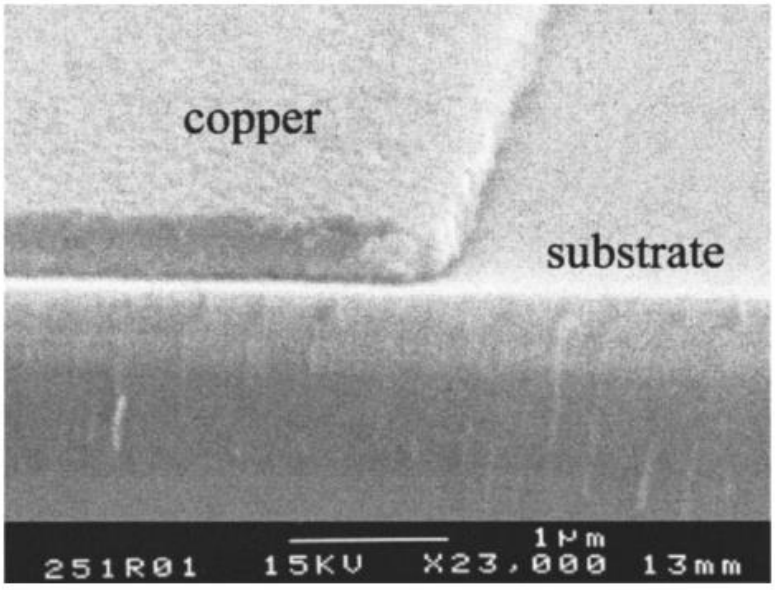

Figure 1.10 Vertical Cu profile after the removal of $CuCl_x$ and photoresist. Reprinted from ref. 16.

Another explanation for this anisotropic etching is the ion bombardment effect. According to Kuo's group previous study [16], during the Cu conversion process, the ion bombardment effect is much deeper than 10 nm because the chlorination reaction can proceed through the whole 500 nm thick Cu layer without stopping. One possible explanation is that the CuClx film was porous, which is easy to transport through by the energized ions. Although the mechanism needs to be further verified, it is clear that ion bombardment is an important factor in this Cu conversion process. The ions and atoms gain momentum on the vertical direction because the applied voltage V_{dc} is perpendicular to the substrate. As the applied – V_{dc} increases, the residue on the bottom is reduced after the HCl dipping. When the -V_{dc} reaches at 250V level, the residue is totally removed for most of the circumstances. Both grain boundaries vertical orientation and the ion bombardment effect could explain why the plasma reaction prefer to occur on the direction perpendicular to the substrate. However, more researches needed to be done to figure out which effect is dominating this mechanism.

If HCl is used as the feeding gas, swelling effect has been detected on the photoresist. According to ref. 16, during the plasma exposure, Hydrogen atoms from HCl can diffuse into photoresist and react with carbon. The reaction between Hydrogen and carbon can form new Hydrocarbon bonds resulting in the photoresist swelling effect. The new polymer formation doesn't have any chemical effect on Cu conversion, because this new polymer is resistant to the HCl plasma and won't induce any extra ions into the chamber. The drawback of the photoresist swelling effect is that the swelling photoresist may block some of the uncover Cu from being etched. When Cl_2 is used as the feeding, photoresist swelling effect is not observed.

Since Br has similar chemical characteristic with Cl, HBr can be used as the substitute for HCl [18]. According to the previous study [18], the swelling effect could also be observed when using HBr as the feeding gas.

In summary, Cl_2 is a better option for the feeding gas than HCl. Because when the gas flow rates are the same, Cl_2 plasma has higher conversion rate than HCl plasma and Cl_2 plasma won't cause swelling effect on the photoresist.

Figure 1.11 shows a 0.8 micrometer Cu line etched by HCl/Ar plasma.

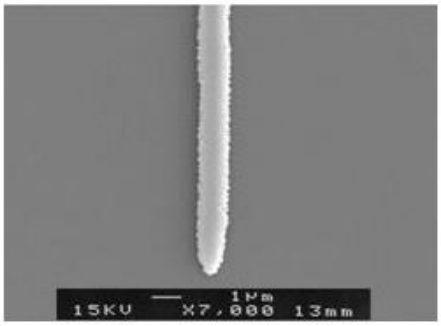

Figure 1.11 A 0.8 micrometer Cu line etched by HCl/Ar plasma. Adapted from ref. 19.

The Cu lines shown in Figure 1.1 has good uniformity. After enlarge, the roughness on the Cu line's side is about 25 nm. Rough lithography and photoresist swelling effect may be the cause of the roughness. With a more exquisite mask and a more accurate mask aligner, the line width can be further narrowed. The roughness on the Cu line sides can also be reduced.

Other gasses besides Ar, have been used to mitigate the sides roughness and the undercut, such as CF_4 and N_2. According to the previous study [20], CF_4 or N_2 plasma reaction with Cu can form a thin film on the Cu line sidewall to protect the sidewall and reduce the undercut problem. The Cu compound formed on the sidewall could be CuN_x or CuF_x, depending on what kind of feeding gas is used. This compound cannot form in the bulk area, because the strong ion

bombardment can breakdown CuN_x or CuF_x immediately once it forms. Figure 1.12 shows the simplified mechanism of the sidewall protection. The actual proportion of each layer is different with the proportion shown in Figure 1.12. Figure 1.12 only shows the mechanism.

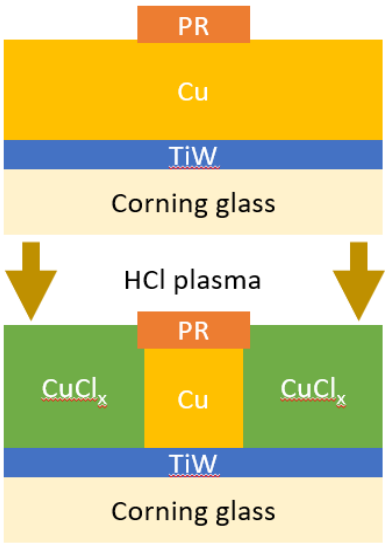

(a) Without CF_4 or N_2 added to the HCl plasma

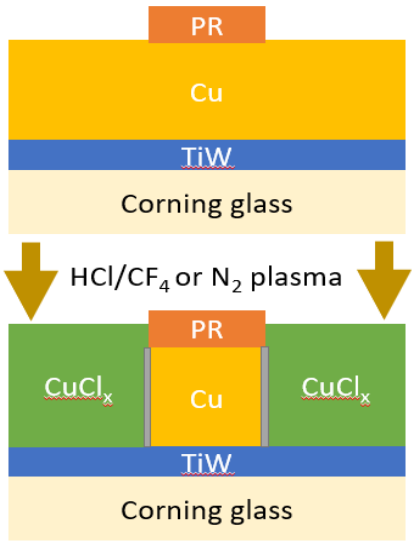

(b) With CF_4 or N_2 added to the HCl plasma

Figure 1.12 Simplified mechanism of the sidewall protection. (a) without side effect protection, (b) with CF_4 or N_2 gas protection.

Figure 1.12 shows that, due to the reaction between Cu and HCl plasma and the $CuCl_x$ swelling effect, there would be slightly undercut on the sidewall of the Cu line.

Using diluted HCl solution to remove the $CuCl_x$, have a drawback of this Cl_2/HCl plasma etching method. When the substrate is made of oxide or metal that can react with HCl solution, the Cu layer may separate from the substrate after dipped in to HCl solution. This etching method could only use to etch Cu that deposited on the substrate cannot react with HCl solution, such as inert metal, silicon and dielectric material. Additional barrier layer is required, if Cu needs to be deposited on the substrate that can react with HCl solution.

1.3.2 Cl_2/HCl plasma etching with H_2 feeding gas

It is difficult to etch Cu with the conventional plasma etching process because it does not form volatile products. Additional energy has to be used to vaporize the Cu compound and the etching process is slow. A modified method, i.e., replacing the HCl solution dip with a H_2 plasma exposure in an ICP reactor to remove the $CuCl_x$, has been reported [21-22]. However, the H_2 plasma need to be carried at a low temperature, e.g., 10^oC, and the $CuCl_x$ removal rate is low. The overall Cu etch rate is about 13 nm per minute. When the sample thickness is 300nm, it will take approximately 20 minutes to finish the etching process. If the plasma system keeps running for more than 20 minutes, the power consumption is high. Besides, low temperature has to be remained during the whole process, which can also consume mass of power. In addition, the hydrogen plasma exposed photoresist is cross-linked and swollen [23], which is difficult to strip with a wet solution.

According to the experiments, after the Cl_2/HCl plasma exposure, when the samples are dipped into high concentration HCl solution, the dipping process usually takes less than one minute. It consumes less time than Cu conversion process. During the whole process, the Cu conversion process will occupy most of the time. The Cu conversion rate is directly related to the substrate temperature due to the reaction kinetics [16]. For instance, When Cl_2 is used as the etching gas, at a 600 W and 20 mTorr plasma condition, the Cu conversion rate is about 600 nm per minutes at the room temperature, which is about 25 °C. When the substrate temperature is higher, the Cu conversion rate will also be higher. When the substrate temperature increases from 25 °C to 100 °C, the Cu conversion rate increases from 600 nm per minute to 1200 nm per minute [16]. The temperature effect is not very obvious. The ions need time to travel to the Cu surface. The ions travel speed is not only related to the temperature. It also related to the applied voltage, so that may explain why temperature doesn't affect the conversion rate much. Combined with the diluted HCl washing process, the whole process will take only 2 minutes for a 500 nm thickness Cu sample. However, it will take about 40 minutes to finish the etching process with the H_2 plasma exposure.

1.4 Cu etching method comparison

Table 1.1 shows the main advantages and disadvantages of different kind of etching methods. After comparing all these Cu etching methods, the Cl_2/HCl plasma conversion with diluted HCl solution removal method has optimum etch rate, can etch both mosaic and salient structures, can be operated with eligible power at room temperature and has only slight undercut. This etching method has no obvious disadvantage and has several advantages when compared with other etching methods, which makes it the most optimum etching method for this research.

Table 1.1 Advantages and drawbacks of different kind of Cu etching method.

Green: advantages Yellow: mediocre Red: disadvantages Blue: undefined

	Etch rate	Structure	Power consumption	Undercut	Environment temperature
CMP	Depending on slurry	Mosaic only	Depending on wafer size	No undercut	Room temperature
$FeCl_3$ wet etching	Very fast (20 μm/min)	Both mosaic and salient	No power consumption	Serious	Room temperature
Cl_2/HCl plasma conversion with H_2 plasma removal	Slow (13 nm/min)	Both mosaic and salient	High power (300-600 W)	Slight	Low temperature
Cl_2/HCl plasma conversion with HCl removal	Optimum (200 nm/min)	Both mosaic and salient	High power (300-600 W)	Slight	Room temperature

1.5 Sample preparation

Two kinds of structures were prepared, Cu lines with TiW barrier layer, and Cu lines not only with the TiW barrier layer but also with TiW capping layer on top. Most of time, the TiW capping layer is used for connecting another layer on top.

In order to observe isolated Cu line electromigration, both two structures were both deposited on the Corning glass, which is a very good heat isolated material. Corning glass is basically made of SiO_2 and SiN_x. If Cu is deposited on the Corning glass directly, poor adhesion and Cu diffusion effect are always two serious problems, so for both two kind of structures, a 10 nm thin TiW film was deposited as barrier layer to enhance the adhesion and prevent the diffusion effect. It is reported that TiW can stand again high temperature and has higher melt point than most of other barrier layer materials [24]. TiW has poor performance when the humidity is high, but in our lab the humidity is extremely low, so TiW is one of the best options.

After barrier layer deposition, Cu was deposited for both two kinds of structures. The deposited Cu film has the polycrystalline structure with the large (111) main peak, a small (200) peak, and a very small (220) peak. In order to observe the relationship between the geometry (which is much larger than the grain size) and lifetime, the average grain size is kept at about 20 nm [25]. It is controlled by the deposition temperature. For lines with TiW capping layer, an additional 10 nm thin TiW capping layer is deposited on the top of Cu layer.

After deposition, two kinds of samples were patterned with a lithography process using a line-and-space mask. Line width of the samples are from 2 μm to 30 μm.

Reactive ion etching method was used to etch pattern samples. CF_4 was used to etch TiW capping layer and barrier layer. HCl plasma was used to etch Cu. CF_4 plasma could convert TiW into gas compound, which can be easily removed from the vacuum chamber. Cu, however, is hard

to form volatile compound. HCl plasma was used to convert Cu into $CuCl_x$. In order to mitigate the sample's undercut, during the Cu etching process, CF_4 gas was added into the chamber to prevent the sidewall from being over etched. Then diluted HCl was used to remove $CuCl_x$.

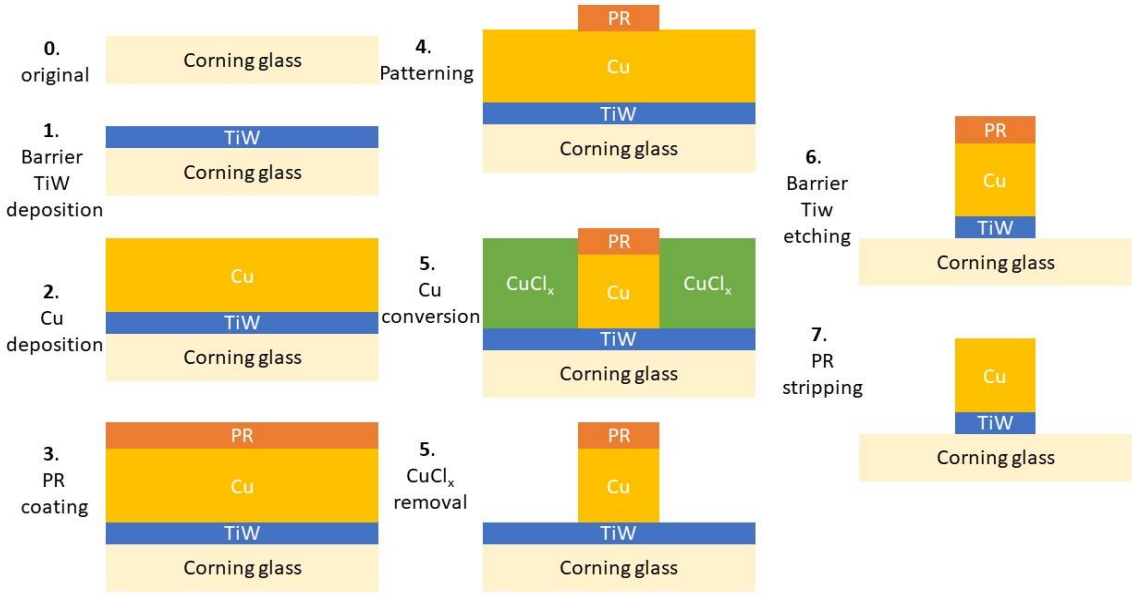

(a)

Fig 1.13 Cu lines deposition and etching process. (a) without TiW capping layer (b) with TiW capping layer.

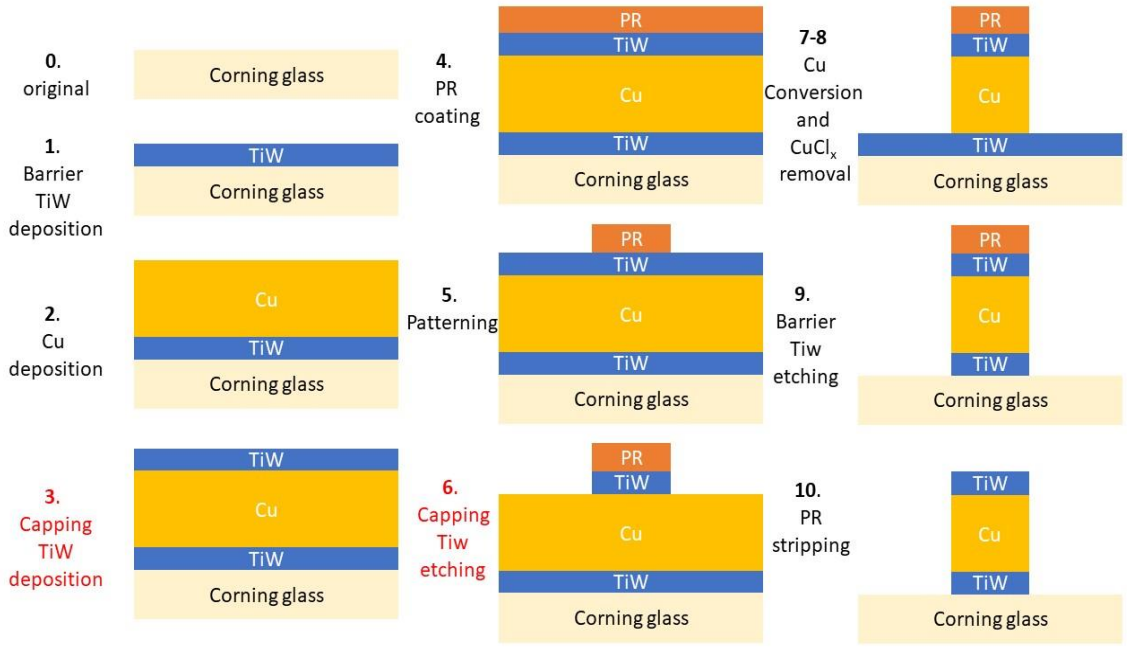

(b)

Fig 1.13 Continued.

Figure 1.13 shows change of the cross-section structure of Cu lines without and with TiW capping layer during the deposition and etching process. For the Cu lines with TiW capping layer, only 2 steps are extra, capping TiW deposition and capping TiW etching. All the other steps remain the same, which can guarantee materials of Cu lines are the same, regardless the structure. The actual proportion of each layer is different with the proportion shown in Figure 1.13. Figure 1.13 only shows the mechanism.

The detailed deposition and RIE conditions could be found in appendix A.

1.6 Electromigration of Cu and Al lines

Electromigration is caused by the momentum transfer from the electrons moving in a wire to the conducting metal atoms. When the voltage is applied to the Cu line, electrons start to flow

through the wire. Some electrons will collide with the Cu atoms. Because of the collision, some Cu atoms are removed from the original place and leave vacancies. Vacancies keep accumulating, until the line breaks down. It was first known 100 years ago. As ICs industry appeared, electromigration started to attract practical interest. Black's equation is first mentioned in late 1960's by Jim Black of Motorola [26],

$$MTTF = \frac{A}{j^n} e^{\left(\frac{Q}{kT}\right)} \tag{1-7}$$

where A is a constant related to the cross-section area, j is the current density, n is a model number related to the temperature, the stress condition and the conducting material, k is the Boltzmann's constant, Q is the activation energy, and T is the absolute temperature in K.

Black's equation has been used to predict lines lifetime for more than 50 years. But back in 1960's, the lines scales were no narrower than 10 μm. Nowadays, as the lines scale keeps shrinking. When it approaches the grain size (20-200 nm), some studies show the black equation cannot fit some circumstances, so research in electromigration area becomes increasingly significant.

Al electromigration has been studied for a long time [27-29]. Back at 1970's, the popular metal interconnect was still Al, so most of the early electromigration test was done on Al lines.

The line width and length effects on Al lines have been studied [30-32]. Since Cu electromigration has similar mechanism with Al electromigration, these previous researches are very helpful to study Cu lines geometry effect. Figure 1.14 shows the relationship between the line width and lifetime.

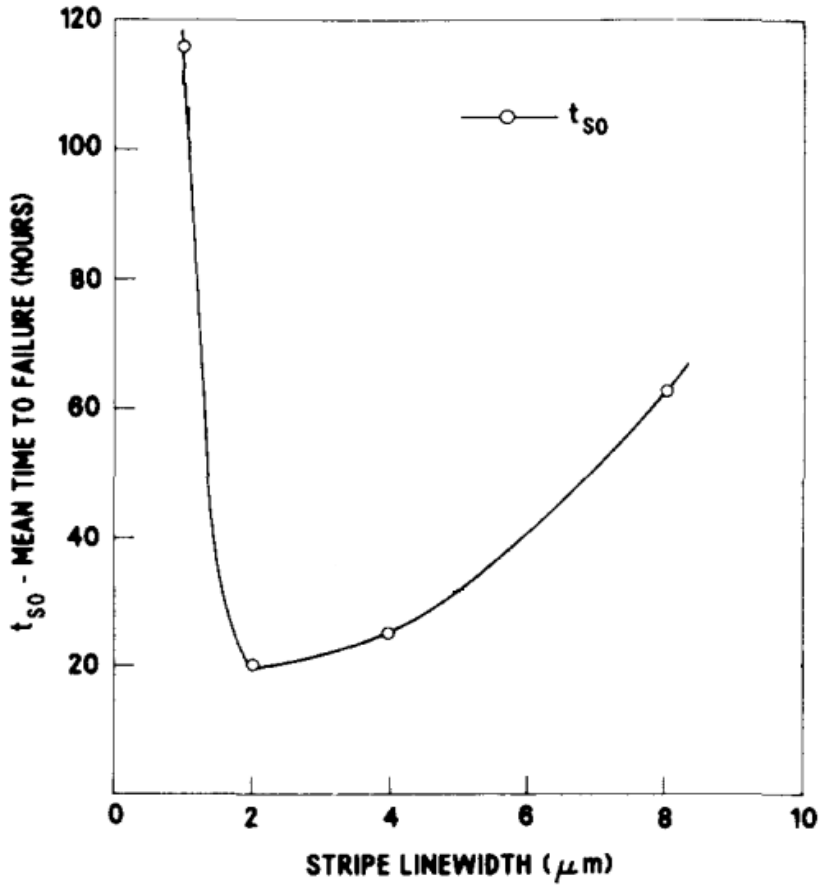

Figure 1.14 Relationship between Al line with and lifetime under the same current density. Adapted from ref. 9.

The grain size of the samples shown in Figure 1.14 is from 2 μm to 5 μm. According to ref. 32 and Figure 1.14, as the width increases, the line lifetime decreases fast when the line width is smaller than 2 μm. However, when the line width is larger than 2 μm, the line lifetime increases. Other previous also show the same trend that line lifetime doesn't have a monotonous relationship with line width. Some researches show the same phenomenon on the relationship between Cu line width and lifetime. One common premise of these previous result is that the grain sizes of their samples have the same scale with the line widths. In this research, Cu grain size is 20 nm [25] which is much smaller than the line width. With this premise, a monotonous relationship between

lifetime and line width has been discovered in this research. Line lifetime decreases as line width increases. This phenomenon will be further discussed in Chapter II.

Also, the line length effect on line lifetime has been studied before. Figure 1.15 shows the relationship between line length and line lifetime under the same current density.

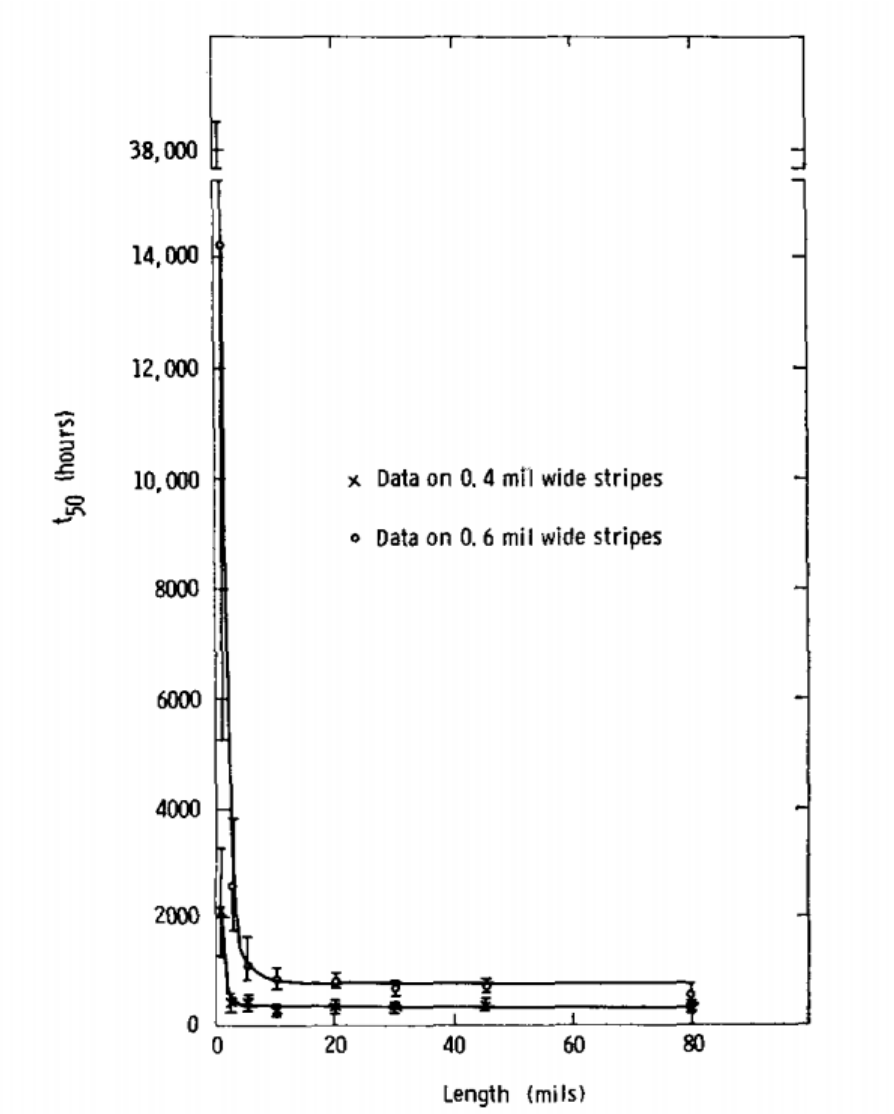

Figure 1.15 Relationship between line length and line lifetime under the same current density. Reprinted from ref. 32.

The grain size of the samples shown in Figure 1.15 still has the same scale with line width, which is about 2 μm. Figure 1.15 shows that line with shorter length has longer lifetime. When the line is shorter than 5 mils, the lifetime decreases dramatically as the line length increases. When the line is longer than 5 mils, the lifetime still decreases as the line length increases, however, the decreasing rate is much slower.

In order to mitigate the electromigration effect and make long life Al lines. Many studies have been done on the Al-Cu alloy electromigration since Cu doping could improve Al lines performance [33-35]. Figure 1.16 shows the relationship between test time and failure chance.

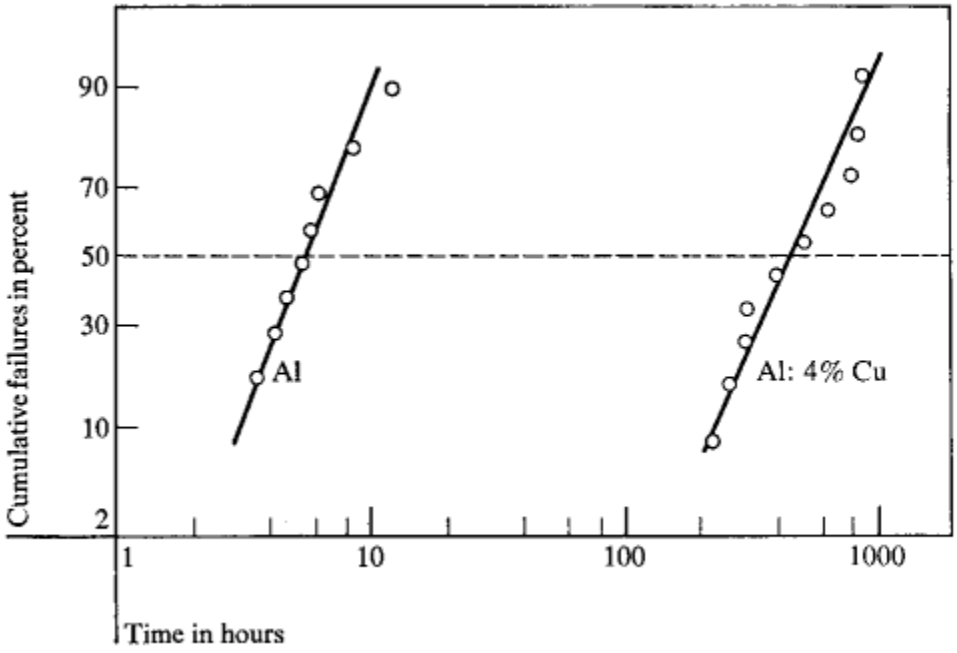

Figure 1.16 Relationship between test time and line failure chance. Reprinted from ref. 16.

Figure shows that, after doping 4% Cu into Al, the Al lines have increased lifetime. The explanation for this phenomenon is that Cu atoms have higher mass than Al atoms, which means, higher electrons drift velocity is needed to cause the same scale electromigration.

The bending effect on Cu lines electromigration test had also been studied before [6]. Figure 1.17 shows the voids formation distribution on part without and with bending effect.

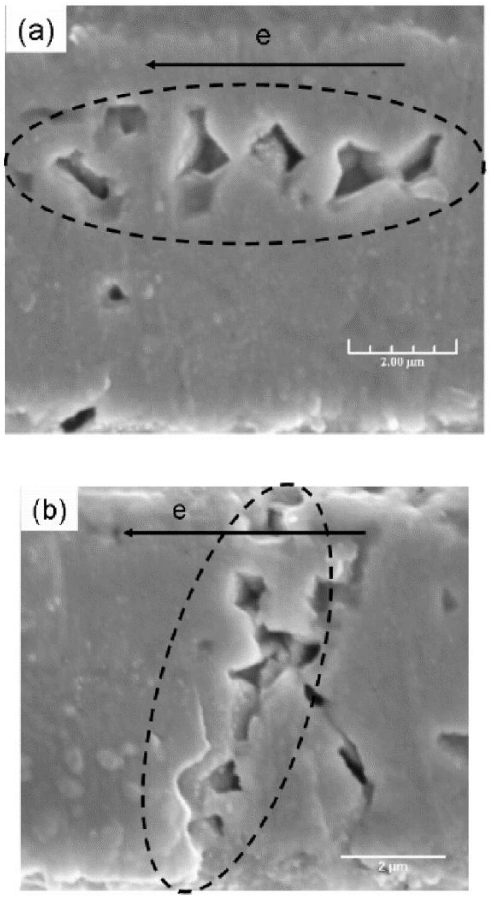

Figure 1.17 Voids distribution in area with and without bending effect. (a) without bending effect, (b) with bending. Reprinted from ref. 6.

Figure 1.17 shows that for lines without bending effect, the voids formation distribution is horizontal with the direction of the current flow. But for lines with bending effect, the voids formation distribution is vertical to the current flow direction, because Cu at the bending point has more fragile structure. With more void formation on the bending point, these voids reduce the effective cross section area of the bending line. However, on the macroscopic view, the same current is still applied. The actual applied current density is higher than before. According to the

Black's equation, higher current density will cause shorter lifetime. This explains why lines with bending effect have shorter lifetime. The line breakdowns fast at the bending point, before other voids can form on the plat part of the line. This explains why voids distribute vertically.

Besides, previous Al lines capping layer effect studies [36] are helpful to the Cu capping layer effect study. Most capping layers can protect the metal from the surface oxidation. Previous study [36] shows that after Al_3Ti deposition, Al lines have increased the lifetime slightly. Figure 1.18 shows the lifetime difference of Al lines with and without Al_3Ti capping layer.

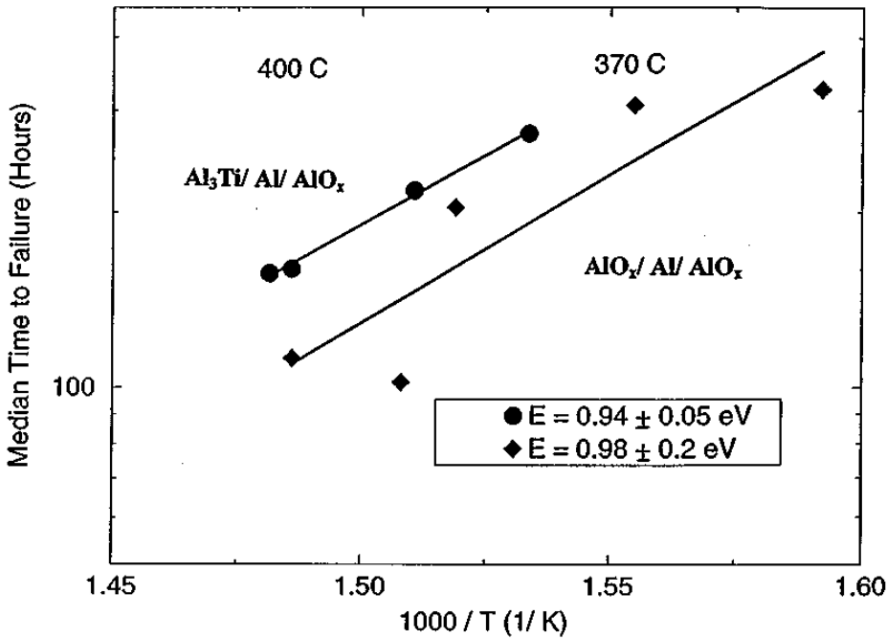

Figure 1.18 Lifetime difference between lines with and without Al_3Ti capping layer. Reprinted from ref. 36.

Figure 1.18 shows that after the alloy capping deposition, the median time to failure has a more linear distribution with 1000/T. The capping layer not only increases the lifetime, but also makes the Al lifetime more predictable.

Similarly, in this research, alloy TiW is deposited on the Cu line to find out if the TiW capping layer has the similar effect on Cu lines.

Most of the recent capping layer effect on Cu lines researches are based on the mosaic structure, which means each side of the Cu line surface, except for the top surface, is attached with other materials, shown as Figure 1.1. Mosaic structure Cu lines are made by chemical mechanical polishing method. Study shows [37], dielectric materials such as SiCN, can increase the line lifetime by preventing the surface oxidation. In this study, capping layer effect on salient structure Cu lines has been studied.

1.7 Electromigration test method and algorithm

For electromigration test, the Cu line failure time was determined by stressing the sample with a constant current density at room temperature until the resistance suddenly jumped by several orders of magnitude or the current loss. Figure 1.19 shows the 4-point test pattern for the EM measurement. A voltage was applied between pads 1 and 2, which was constantly adjusted with a computer program to keep the current at a steady value. The resistance of the Cu line was calculated from the voltage drop between pads 3 and 4 at the steady current.

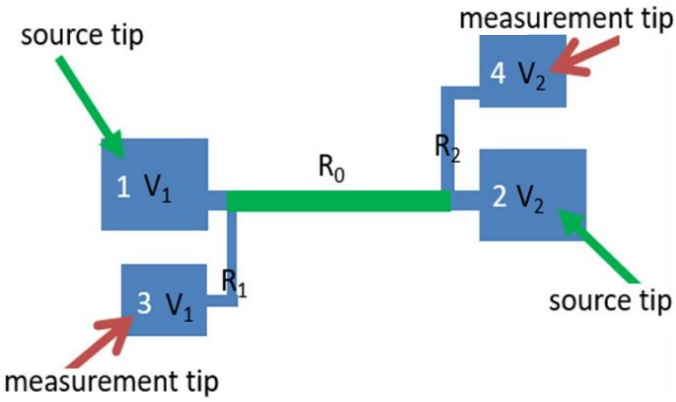

Fig 1.19 A 4-point electromigration test pattern. Reprinted from ref. 38.

The program used to process the electromigration test is based on Labview. The structure detail of the Labview program is in Appendix B. Table 1.2 shows the essential input/output parameters when a 0.6×10^6 A/cm^2 current density is applied to a Cu lines with width of 1.5 μm and length of 20 μm. Figure 1.20 shows flow chart of the EM test process.

Table 1.2 Essential input/output parameters.

Parameters	Input	Output
Line width (μm)	1.5	
Film thickness (μm)	0.18	
Line length (μm)	20	
Current density (MA/cm^2)	0.6	
Voltage level (V)	0.5	
Voltage limit (V)	30	
Failure criteria	1000	
Maximum R allowed		8312.72
Current limit (A)		1.62m
R measurement		8.29079
Voltage monitoring		0.014696
Current monitoring		1.77m

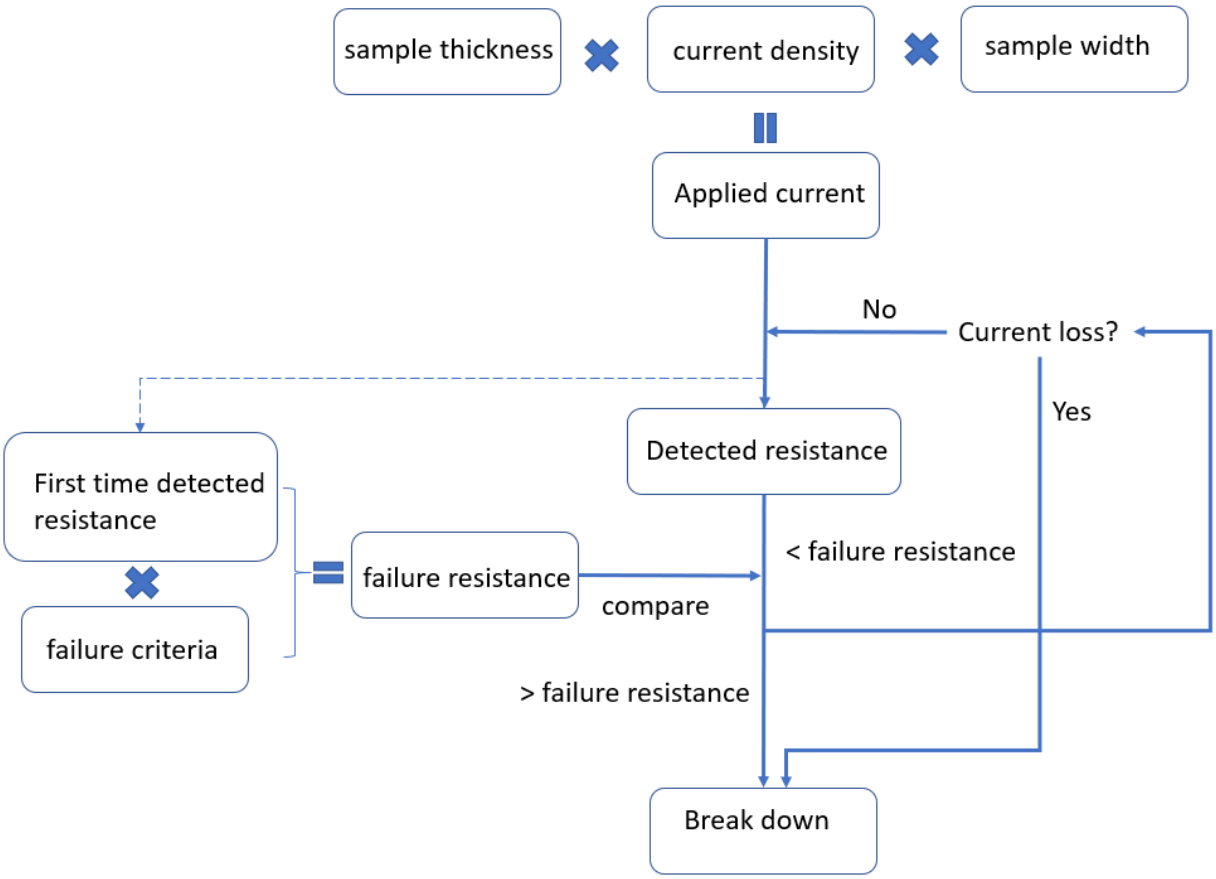

Figure 1.20 Program flow chart of the EM test process.

Figure 1.20 shows that the applied current is calculated by the input sample thickness, current density and sample width. After the current is applied to Cu line, Cu line resistance is detected. The first-time detected Cu line resistance is recorded as the initial resistance. The failure resistance is calculated by multiplying the initial resistance and the input criteria. When the detected resistance is smaller than the failure resistance, the program keeps running. Each time period is set as 1 second. After each time period, the Cu line resistance may have some change when compared with the last period. When the detected resistance is larger than failure resistance, the program will report the breakdown and stop running.

Sometimes, current loss may happen suddenly without detecting the resistance is higher than the failure resistance. Because the test period is set as 1 second, when resistance increases to infinity in less than 1 second, the system is unable to detect it. So, another judging point is set to detect whether there is a current loss.

Line width, film thickness, current density and failure criteria are the essential input factors. They control the applied current density and what is the break down critical point. Without these factors the program cannot work.

The line length factor doesn't affect much of the program. It doesn't change the current density and any other important factors. The voltage level represents the initial voltage applied to the Cu line. After the initial voltage is added, the program will detect the resistance. According to the detected resistance and input current factor, program calculates the correct voltage should be applied. The value of the initial voltage should have similar value as the one when the required current is applied. If the initial voltage is too high, the line may break down immediately. The voltage limit factor keeps the device safe. When an over limit voltage is detected, the program will stop to protect the system from overheat.

2. LINE GEOMETRY EFFECT ON LIFETIME OF PLASMA ETCHED COPPER LINE

2.1 Line width and length effects on EM failure time

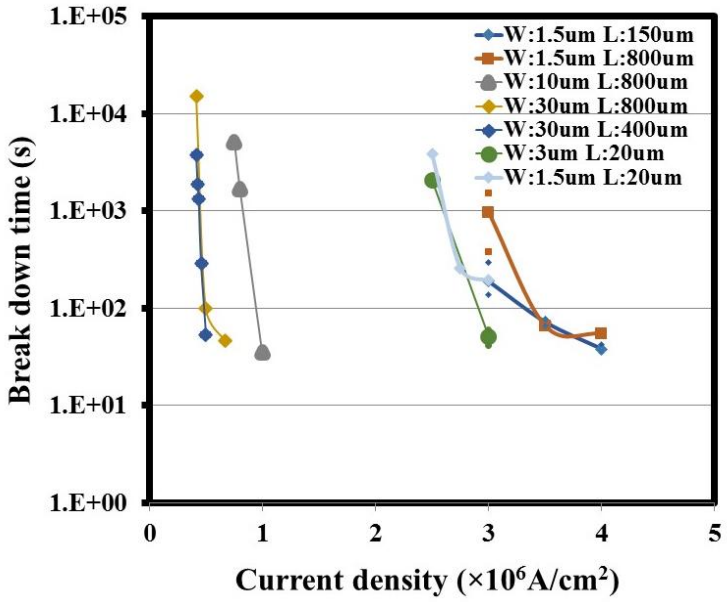

Fig. 2.1 Line broken time vs. current density for Cu lines of various lengths and widths. Reprinted from ref. 38.

Figure 2.1 shows the relationship between the line width W or length L and the EM failure time at various current densities. Several conclusions can be summarized from this figure. First, the line failure time is consistently shortened with the increase of the current density. Second, under the same current density, the narrow line has a longer lifetime than the wide line. Third, the influence of the line length to the failure time is dependent on the line width. For the 30 μ wide lines, the 800 μ long line has a slightly longer lifetime than that of the 400 μ long line. However, for the 1.5 μ wide lines, the 20 μ long line has a lifetime similar to that of the 150 μ long line at the current density of 3×10^6 A/cm^2.

The grain size and grain boundaries intersection points distribution may be the reason of the longer lifetime of the narrow line than that of the wide line under the same stress current density

condition. According to ref. 38, electrons transferred through grain boundaries have higher momentum than through the bulk of the grain. According to previous studies [39,40], EM could be described as the mass flux J expressed below:

$$J = -\frac{N_A}{k \cdot T} \cdot D_0 \cdot e^{-\frac{Q}{kT}} \cdot e \cdot Z^* \cdot \rho \cdot j \qquad (2\text{-}1)$$

where N_A is the density of lattice atoms, D_0 is the diffusion coefficient, Q is the activation energy, $e \cdot Z^*$ is the effective charge, ρ is the specific resistance, j is the current density, k is Boltzmann's constant, and T is temperature (K). At the grain boundary, the diffusion coefficient is large and the mass flux is high. Therefore, atoms at grain boundaries especially at intersection points are subject to the bombardment of the high electron flux. Voids and hollows are formed at these locations, which initiates the electromigration failure process. Sizes of voids and hollows grow with the stress time until the whole line is broken.

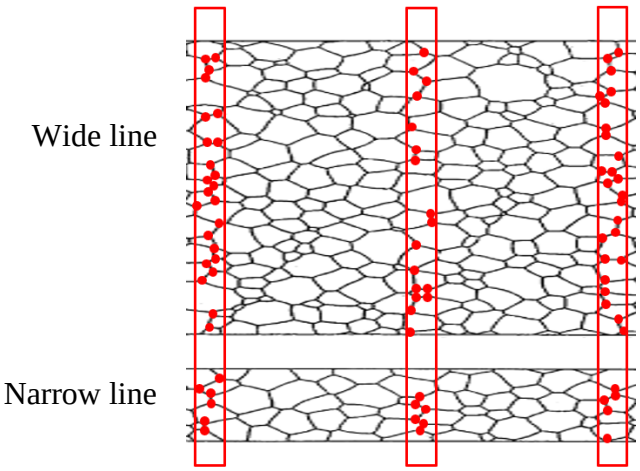

Fig 2.2 Distributions of grain boundary intersection points in wide and narrow lines. Reprinted from ref. 38.

Figure 2.2 shows distributions of grain boundary intersection points in wide and narrow lines assuming both have the same distribution of grains. Some of the intersection points are marked as red dots in Figure 2.2. Under the same current density, it is assumed that all these red dots have the same chance to fail, also the failure chance increases as time increases [5]. Since the wide line has more intersection points than the narrow line, the void's formation has higher chance to appear earlier in wide line.

The line width effect on the EM failure of the Al line has been investigated [8]. In specific range, the narrower line has a longer lifetime than the wide line, which is similar to the result of Figure 2.1 Others had observed the same trend on Cu lines [10,11].

For our samples, the grain size in the Cu thin film is about 20 nm [25]. It is assumed that the film has the uniform columnar grain structure across the whole line. For a 1.5 μ wide line, on the average, there are about 75 grains boundary intersection points at each line location. For a 10 μ wide line, there should be 500 intersection points at each line location. Then, the narrower line has less chance to fail from the current crowding at grain boundary intersection points. Separately, the relationship between the Cu grain size and the lifetime has been reported [25, 41]. The lifetime of the Cu line can be extended when it is composed of larger grains, because larger grains potentially reduce the intersection points.

2.2 Line width and length effects on line resistance

Fig 2.3 shows curves of resistance vs. stress time of Cu lines of various widths and lengths at different current densities. Fig 2.3(a) shows the result of Cu lines of the same W/L 10 μ/800 μ but stressed with different current densities, i.e., 10^6 A/cm^2, 0.8×10^6 A/cm^2, and 0.75×10^6 A/cm^2. The line resistance increases little with the increase of time at the beginning. At near the breakdown

point, the resistance increases abruptly. Besides, the breakdown time increases with the decrease of the stress current density. Fig 2.3(b) shows the similar result on Cu lines of the same line length but different line width from that of Fig 2.3(a) samples, i.e., W/L 30 μ/800 μ vs. 10 μ/800 μ. Samples were also stressed with three different current densities, i.e., 0.67×10^6 A/cm^2, 0.5×10^6 A/cm^2, and 0.417×10^6 A/cm^2. Fig 2.3(c) shows the result of Cu lines of the same line width but different length from that of Fig 2.3(a) samples, i.e., W/L 10 μ/400 μ vs. 10 μ/800 μ, with four different current densities, i.e., 0.5×10^6 A/cm^2, 0.458×10^6 A/cm^2, 0.4375×10^6 A/cm^2, and 0.417×10^6 A/cm^2. The influence of the current density on the line breakdown time is similar with that of Fig 2.3(a) or (b). Fig 2.3(d) shows the result of narrow and short Cu lines, i.e., W/L 3 μ/20 μ, stressed at 2 different current densities, i.e., 2.5×10^6 A/cm^2 and 3.0×10^6 A/cm^2. Again, the same result, i.e., shorter lifetime for the high current density stress condition, is observed. Fig 2.3(e) shows the result of the very narrow Cu lines, i.e., W/L 1.5 μ/150 μ, stressed with three different current densities, i.e., 3.0×10^6 A/cm^2, 3.5×10^6 A/cm^2, and 4.0×10^6 A/cm^2. In addition to the same result that Cu stressed at the low current density has a long lifetime, another phenomenon is observed. Under the low current density stress condition, the resistance changes little with time until reaching the broken point where the resistance abruptly increased. Under the high current density stress condition, the resistance increased with time appreciably even before reaching the broken point. Fig 2.3(f) shows the same result as that of Fig 2.3(e) except the Cu line had a longer length, i.e., W/L 1.5 μ/800 μ vs. 1.5 μ/150 μ, and two different stress current densities, i.e., 3.0×10^6 A/cm^2 and 3.5×10^6 A/cm^2, were used. The line resistance changed little until it broke sharply.

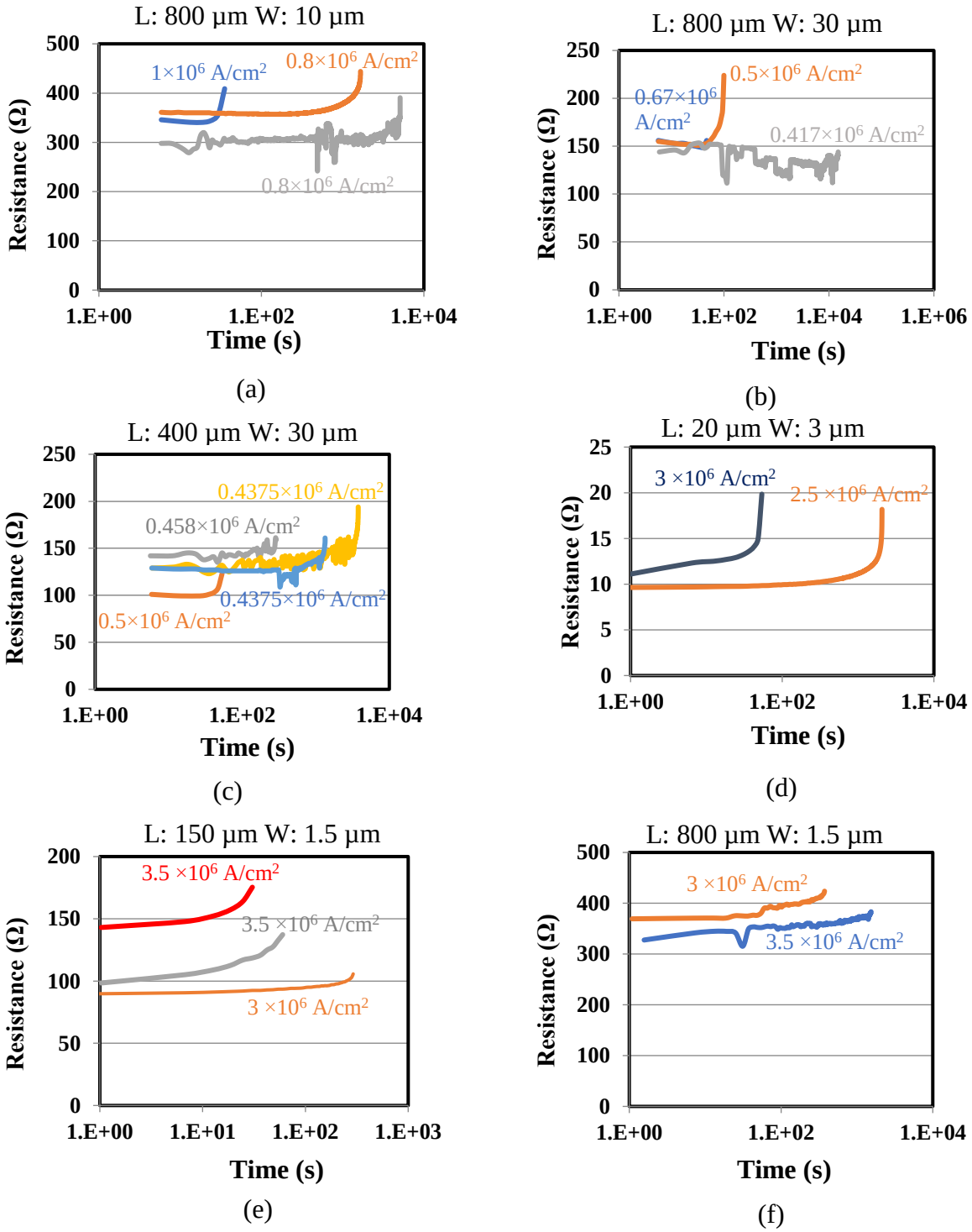

Fig 2.3 Cu line resistance change with stress time. (a) W/L 10 µ/800 µ, (b) W/L 30 µ/800 µ, (c) W/L 30 µ/400 µ, (d) W/L 3 µ/20 µ, (e) W/L 1.5 µ/150 µ, (f) W/L 1.5 µ/800 µ. Adapted from ref. 38.

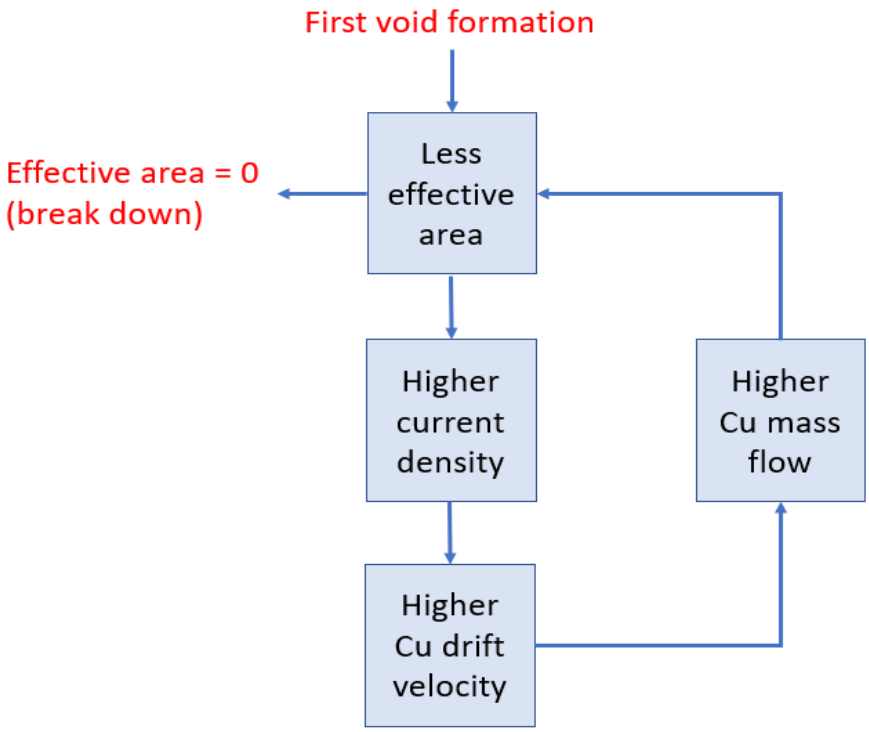

Fig. 2.4 lines breakdown mechanism under constant current density.

Figure 2.4 shows how lines breakdown because of the voids' formation and actual current density change. After the first void has formed, the effective cross section area (area that electrons can pass through) decreases, but from the macroscopic view, the applied current remains the same. So according to $J = \frac{I}{A}$, the actual current density increases. According to mass flux J equation, higher current density can cause higher mass flow. Higher Cu mass flow induces more voids into the Cu lines, which can further decrease the effective cross section area. This loop keeps running until the last point on this cross-section area fails.

Fig 2.3(a) and Fig 2.3(f) show that the narrow line breaks down more abruptly than the wider one. For the one-unit width line, once there is a point failure, the line resistance will increase from normal to infinity instantly. For the wider lines, however, one-point failure will not cause the break down immediately. It will increase the resistance gradually, so the loop shows in Figure 2.4

can sustain for a longer time than the narrower line can. This explain why the wider lines have smoother resistance profile than the narrower lines before breakdown.

Fig 2.3(e) and Fig 2.3(f) show that, for lines of the same width, the longer lines show more abrupt resistance change before break down than the shorter lines do. The shape of the resistance vs. time curve is related to the temperature of the Cu line, which is width-, length- and current density-dependent.

Figure 2.5(a) shows the 100× magnification image of a W/L 30 μ/400 μ Cu line that was broken under EM at the current density of 0.3×10^6 A/cm^2. Most of the line changed color symmetric to the broken point. Macroscopically, the width of the line remained unchanged even at the broken point. Fig. 2.5(b) shows the 100× magnification image of a narrow and long W/L 10 μ/800 μ Cu line that was EM stressed at the current density of 0.8×10^6 A/cm^2. Although this line was not broken, it narrowed apparently at 2 separate places where the color changed dramatically. Since the narrow line contains a few grain boundary intersection points, the EM failure may occur randomly, which is different from that of the wide line. When the lines were further narrowed, the pattern of the EM broken line became uneven. Fig. 5(c) and (d) show 100× and 1,000× magnification images, separately, of a W/L 1.5 μ/800 μ Cu line broken from a stress current density of 0.3×10^6 A/cm^2. In both figures, most area of the line had the same color except at the broken point. Therefore, the failure of the very narrow line probably occurred at the weakest point locally rather than randomly.

The uneven electromigration distribution could also explain why the narrower line has a more abrupt resistance profile before break down. For the wider lines, most of parts have increased the resistance because of the electromigration. The total resistance of the wider line has already increased a lot right before break down. For the narrower line, only the part near the break down

point has increased its resistance because of the uneven distribution of electromigration. The total resistance of the narrower line hasn't increased a lot right before break down. When the break down happens on the narrower line, the resistance increases from its normal value to infinity suddenly.

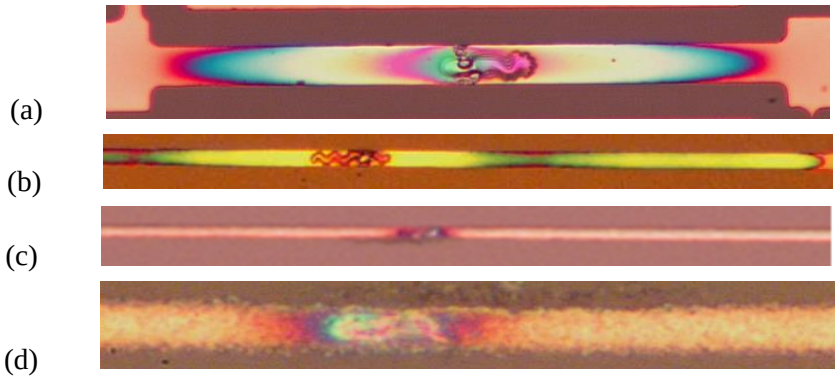

Fig 2.5 Images of EM broken lines. (a) W/L 30 μ/400 μ, J = 0.3×10^6 A/cm^2, 100× magnification, (b) W/L 10 μ/800 μ, J = 0.8×10^6 A/cm^2, 100× magnification, (c) W/L 1.5 μ/800 μ, J = 3×10^6 A/cm^2, 100× magnification, (d) W/L 1.5 μ/800 μ, J = 3×10^6 A/cm^2, 1000× magnification. Reprinted from ref. 38.

The uneven electromigration distribution could also explain why longer line has a more abrupt resistance profile before break down. For the longer line, the electromigration break down area only occupies a few percentages of the total area. For the shorter line, however, the break down area occupies most of the area. This also means that electromigration happens more evenly in the shorter line that in the longer line. The same mechanism will lead to the same effect that the longer line has more abrupt resistance profile than the shorter line.

2.3 Conclusion

The narrow Cu line has a longer EM lifetime than the wide line when stressed under the same current density, which can be explained by the grain boundary intersection points effect.

From the resistance vs. time curve, the narrow line breaks down more abruptly than the wide line because electromigration happens unevenly in the narrow line. At the location of the electromigration failure point, the local resistance changes drastically. Therefore, when the narrow line is broken, a large portion of the line still remains low resistance. For the wide line, electromigration happens evenly. The resistance of most part of the line changes little with the stress time until the whole line is broken. Patterns of the broken lines show that for the wide line, the color changes even along the line. As the line is 10 μ wide, the color change along the line is random. When the line width is further reduced to 1.5 μ, the color change becomes more uneven. The EM lifetime of the Cu line is related to the distribution of the grain boundary intersection points and the grain size. Therefore, the grain structure of the Cu line is important to the EM lifetime.

In the previous studies, the Cu grain size is on μm scale, which is similar with the line width. Some of the lifetime tests result show that the narrower line has shorter lifetime when the line width is too narrow. This is because when the line width is narrower than the grain size, the grain structure turns into bamboo structure, shown in Figure 2.8 (b).

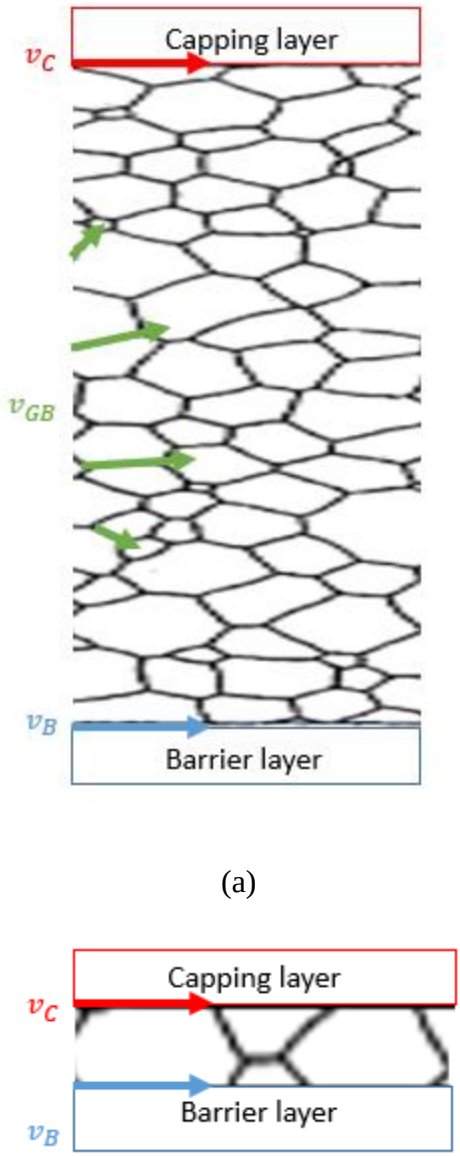

(a)

(b)

Figure 2.6 Electrons flow path for different grain structure. (a) grain size is much smaller than the line geometry scale, (b) grain size is approaching or larger than the line geometry scale (bamboo structure).

Figure 2.6 shows different electrons flow path of Cu lines with different grain structure. When gain size is approaching or larger than the line geometry scale, the electrons can no longer travel through the grain boundaries. In the bamboo structure, because there are only few electrons

travel through the grain boundaries and there are not many grain boundaries intersections. Most of the electromigration may not happen at the intersection points. The electromigration failure mechanism is totally different and cannot be explained by the intersection points distribution theory mentioned in this research.

This study first reveals that, when the grain size is much smaller than the line width, electromigration prefer to happen at the grain boundaries intersection points, which will lead to the fact that wider line has shorter lifetime than narrower line. Cu grain size has significant effect on the relationship between Cu lines width and lifetime. Grain size and line width should be considered together. When the line width has the same scale with Cu grain size, there may be more than one electromigration break down mechanisms. In this study, Cu size is limited under 20 nm, which is much smaller than the Cu line width. The grain boundaries intersection points distribution is the dominate mechanism to explain why wider lines have shorter lifetime.

3. CAPPING LAYER EFFECT ON LIFETIME OF PLASMA ETCHED COPPER LINE

3.1 Capping layer effect on EM line broken time

Figure 3.1(a) shows curves of the line broken time vs. stress current density of TiW capped and noncapped Cu lines of different widths. Samples were of the same length of 800 μm but different widths of 10 μm, 30 μm, or 2.5 μm. First, the line broken time reduced with the increase of the current density. This is consistent with the previous report that the lifetime decreased with the increase of the stress current density exponentially [5]. Second, the 30 μm wide line has a shorter lifetime than the 10 μm wide line independent of the existence or absence of the TiW capping layer. This is also consistent with our previous observation that wide lines are subject to earlier failure than narrow lines due to the higher opportunity of forming voids at the larger number of grain boundaries [38]. Third, based on the same line width, Cu with a TiW capping layer has a shorter lifetime than that without the capping layer. According to a previous study [42], the capping layer might induce void defects in the Cu layer, which could shorten the EM lifetime.

Figure 3.1(b) shows the same data as Figure 3.1(a) expressed as the mean time to failure (MTTF) vs. current density. The following modified Black equation was used to fit each curve [26],

$$MTTF = \frac{A}{j^n} e^{\left(\frac{Q}{kT}\right)} = A \cdot e^{-n \cdot lnj + \frac{Q}{kT}} = C \cdot e^{-n \cdot lnj} \quad (3\text{-}1)$$

where A is a constant related to the lines structure, j is the current density, n is a model number related to the temperature, the stress condition and the conducting material, k is the Boltzmann's constant, Q is the activation energy, and T is the absolute temperature in K, and C is a constant dependent on A, Q and the absolute temperature T ($C = A \cdot e^{\frac{Q}{kT}}$).

In Fig 3.1(b), the *n*-values of lines with same width are almost the same. The capping layer has no obvious effect on the *n*-value. For the 30 μm and 2.5 μm wide lines, the *n*-values are 4.25-5.64. For the 10 μm wide lines, the *n*-values are 1.1-1.36. According to the recent study [43] on the temperature effect during the EM test, it shows that the temperature changes for both two kinds of structure are almost the same. This is because the capping TiW layer is only 10 nm, which is much less than the thickness of Cu layer (280 nm). The main part of the Cu line is still made of Cu. The temperature change rate won't change much for the same kind of material.

For the lines with same width, samples without the thin TiW capping layer have a larger *A*-factor and therefore, a longer broken time. However, it was reported that the Black equation did not consider factors such as the temperature gradient and Joule heating effect [44]. They might lead to the inaccurate *n*-and *A*-values.

Separately, it was reported that the temperature of the Cu line was increased by the EM stress [44-46]. At high temperature, Cu could easily diffuse into the TiW capping layer [24]. Once Cu atoms are lost to the adjacent layer, voids could be formed in the bulk Cu line. In previous studies on the relationship between the Cu vacancy and diffusion [47-48], it was found that the increase of vacancy could enhance the Cu diffusion rate. Vacancies could even change the shape and location of the local grain boundaries [49]. The following equation, which has been mentioned in Chapter 1, expresses the mass flux under the EM condition [39, 40].

$$J = \frac{N_A}{kT} \cdot D_0 \cdot e^{\left(-\frac{Q}{kT}\right)} \cdot (e \cdot Z^*) \cdot \rho \cdot j \qquad (3\text{-}2)$$

When the diffusion constant increases, the mass flux *J* increases. Then, the electromigration phenomenon becomes serious and the Cu line lifetime is shortened.

(a)

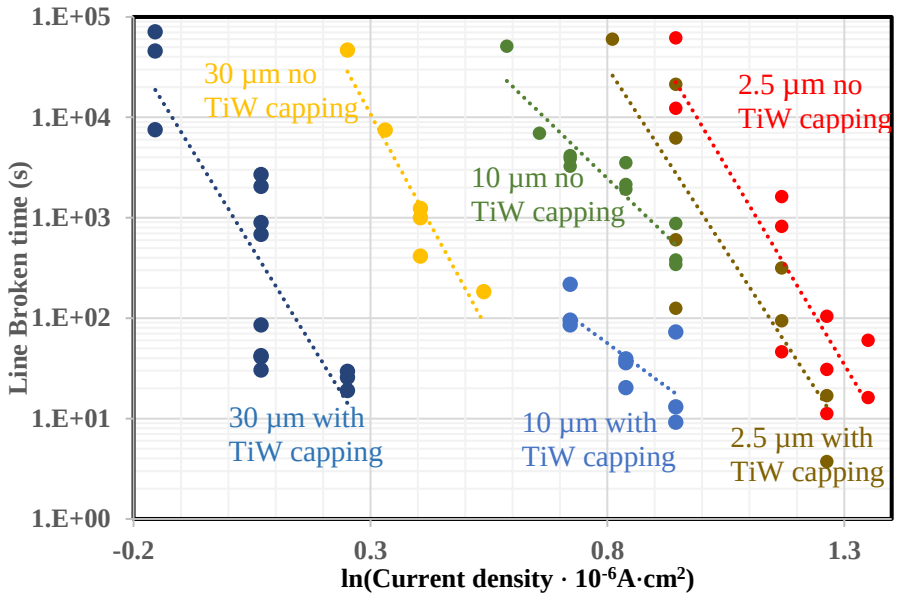

(b)

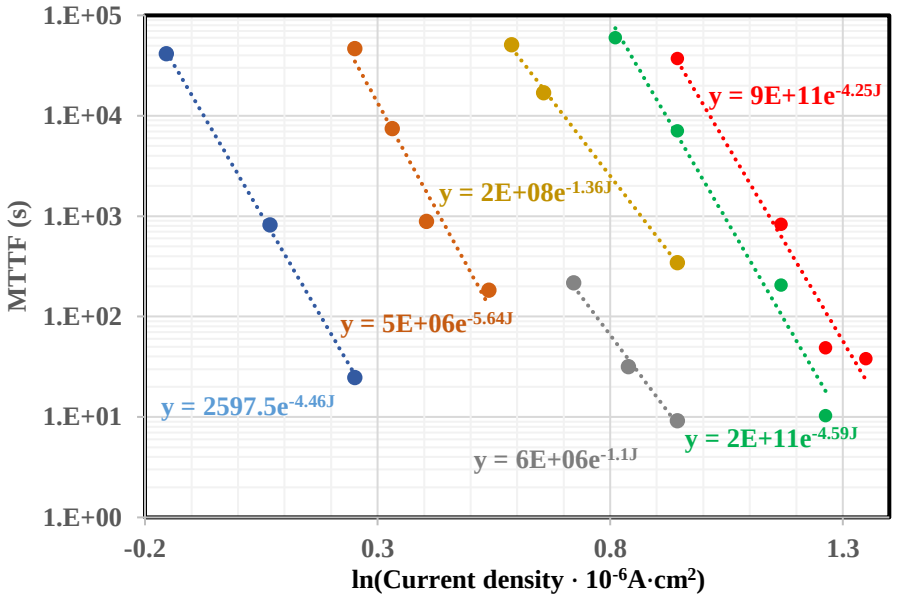

Fig 3.1 (a) 'Line broken' time vs. stress current density of TiW capped and uncapped Cu lines of different widths and (b) MTTF vs. current density of (a) samples fitted with Black equation. Reprinted from ref. 50.

The color of the TiW capped Cu line changed with the EM stress time. The original line color was purple, as shown in Fig 3.2(a). It changed to the white color, as shown in Fig 3.2(b),

where the broken area showed as the dark color. Since the reflection of the light from the surface is dependent on the composition of the TiW capping layer, the color change may be related to its composition change. Table 3.1 shows the XPS elemental ratios of the TiW capping layer before and after the line broken. The W/Cu and Ti/Cu ratios decreased after the EM stress while the Ti/W ratio remained the same. Therefore, Cu was diffused into the TiW layer during the EM stress. The shortening of the line broken time from the addition of the TiW capping layer can be explained by the loss of Cu atoms in the bulk Cu line.

(a) (b)

Figure 3.2 Light microcopy images showing the color of a 30 μm wide TiW/Cu/TiW line. (a) before and (b) after line broken from EM stress at $J = 1.39\times10^6 A/cm^2$. Reprinted from ref. 50.

Table 3.1 XPS elemental ratios of TiW capping layer before and after EM stress. Reprinted from ref. 50.

	Before	**After**
Ti/Cu	3.5	3.4
W/Cu	18.9	17.7
Ti/W	0.19	0.19

3.2 Capping layer effect on Cu line resistance

Figure 3.3(a) shows the resistances of 10 μm lines with and without TiW capping layer vs. the EM stress time at $J = 2.06\times10^6 A/cm^2$. First, the resistance of the line changed little with increasing time until near the broken point. Second, the resistance of the sample with TiW capping layer is larger than that without the capping layer. According to previous studies [51-53], for Cu lines with the capping layer, EM prefers to happen at the interface. At the interface, Ti-Cu or W-

Cu bonds provide lower conductivity than Cu-Cu bonds, which causes the larger resistance. Third, for lines without TiW capping layer, the broken phenomena occurred earlier than those without the TiW capping layer. This can be explained by the easy formation of voids in the bulk Cu line from the loss of atoms to the capping layer.

Figure 3.3(a) shows the resistance vs. EM stress time curves of the TiW capped and uncapped 10 μm lines at $J = 2.06\times10^6 A/cm^2$. Figure 3.3(b) shows the resistance vs. EM stress time curves of the TiW capped and uncapped 2.5 μm lines at $J = 2.57\times10^6 A/cm^2$. Similar with the 10 μm lines, the TiW capped lines have larger resistance than the uncapped lines. For both samples, the line resistances change slightly with the increase of the stress time until near the broken point.

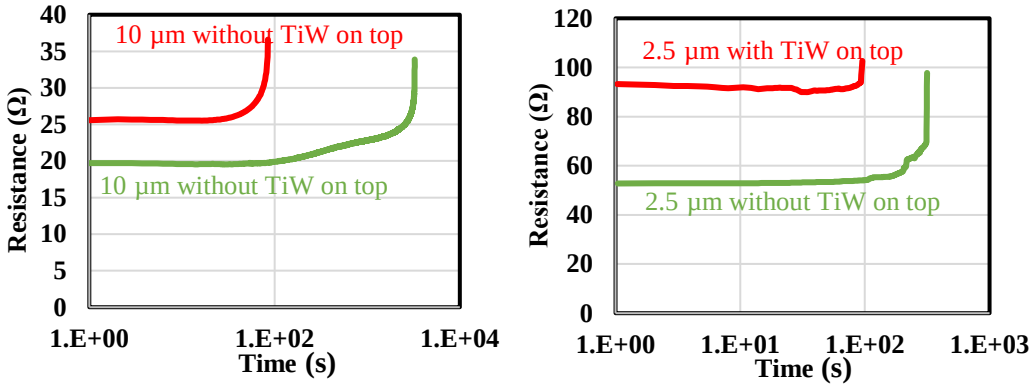

(a) (b)

Fig 3.3 Line resistance vs. stress time of TiW capped and uncapped Cu lines. (a) 10 μm line at $J = 2.06\times10^6 A/cm^2$, (b) 2.5 μm line at $J = 2.57\times10^6 A/cm^2$. Reprinted from ref. 50.

Fig 3.4 shows the difference of resistance and cross section area for two kinds of structure. Both cross section area and resistance of Cu lines with TiW capping layer are larger than the uncapped lines. The power consumption can be calculated by the following equation.

Lines without capping layer: $P = I^2R = (aj)^2R = a^2Rj^2$ (3-1)

Lines with capping layer: $P_{Capping} = I_{Capping}{}^2R = (a + \Delta a)^2(R + \Delta R)j^2$ (3-2)

The Cu layer thickness is 280 nm, which is much thicker than the capping layer (10 nm), so when the power consumption is calculated, the cross-section area part doesn't attribute much increase because the cross-section only increases about 3-4%. According to Fig 3.3(a), the resistance of 10 μm width line increases about 25% after the line is capped. For the 2.5 μm width line, the resistance increases even more. The final consequence of higher resistance and larger cross-section area is that, when the same current density is applied, lines with capping consume at least 25% more power than the uncapped lines. As mentioned before, these lines were deposited on the corning glass, which is a very good heat isolated material, so the applied power keeps accumulating on the Cu lines until they break down. For the lines with capping layer, the Cu atoms not only diffuse into an additional layer (TiW capping layer), but also diffuse at a higher rate because more heat is accumulated during the EM test, shown as Fig 3.5.

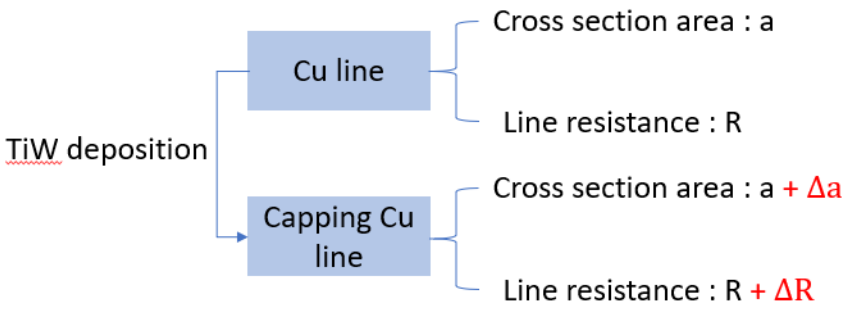

Fig 3.4 Resistance and cross area difference between Cu lines with and without TiW capping layer.

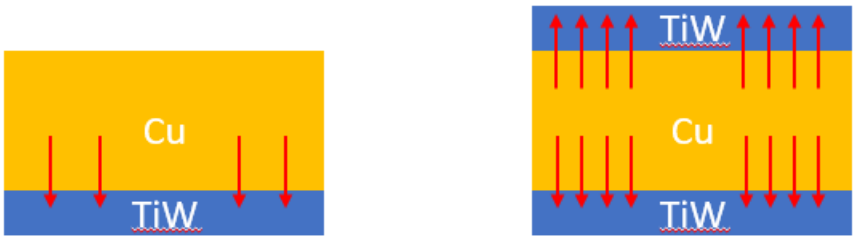

Fig 3.5 Cu atoms diffusion direction and rate for both two kinds of structure.

3.3 Conclusion

The TiW capped Cu line has a shorter ‘broken line’ time than the uncapped Cu line. This can be explained by the loss of Cu atoms to the TiW layer during the EM stress. This phenomenon causes the enhancement of the vacancy formation and the acceleration of the line disruption. The raise of temperature during the current stress also enhances the mass flux at the junction point that results in the early failure of the line. The resistance vs. stress time result shows that the TiW capping layer causes an increase of the line resistance leading to void formation in the bulk Cu line. Thus, the selection of the capping layer material is critical to the electromigration failure of the Cu line.

This research shows that sometimes the capping layer could reduce the Cu lines lifetime instead of increasing it. During the electromigration, surface of the Cu lines without capping layer have the oxidation problem. Oxidation reduces Cu lines lifetime seriously. In common situation, capping layer is usually designed to protect the surface from oxidation. However, diffusion effect has been observed in this research. The capping layer does reduce the oxidation on the Cu lines surface during the electromigration test, but the diffusion effect from Cu layer to TiW barrier layer makes the capped Cu lines have shorter lifetime than the uncapped Cu lines.

4. SUMMARY AND CONCLUSIONS

When the same current density is applied, the wider Cu line has a longer EM lifetime than the narrower line, which can be explained by the grain boundary effect. According to the resistance and time relationship profile, the narrow line's curve is more abrupt right before break down because of the uneven distribution of electromigration in the narrow line. At the electromigration break down point, the resistance increases drastically. However, a large portion of the line still remains low resistance. The electromigration happens more evenly in the wide line. Most part of the line resistance has increased before the break down happens. Picture of the broken wide line (30 μm) shows the color changes evenly along the line. For the 10 μm line, the color change distribution is not as even as the 30 μm ones, but most portion of the line still changes the color. When the line width is further reduced to 1.5 μ, the color change only happens at the area nearby break down point. The EM lifetime of the Cu line is related to the distribution of the grain boundary intersection points and the grain size. Therefore, the grain structure of the Cu line is important to the EM lifetime.

In order to extend the lifetime of Cu lines without capping layer, annealing is a good option. Cu annealing could increase the Cu grain size and reduce the Cu grain boundaries intersection points, where the voids prefer to form during electromigration. In specific application, when constant current density is required in circuit, narrower Cu lines have longer lifetime. When constant current is required in circuit, using multiple narrower Cu lines to replace one wider Cu line might increase the overall lifetime. However, according to the previous studies, sometimes when the line is too narrow, the lifetime will also be reduced under the same current density. This research shows that reducing the line width will increase the life time, as long as the line width scale is larger than the grain size.

Cu line without TiW capping layer has a longer lifetime than the TiW capped Cu line, which can be explained by the loss of Cu atoms to the adjacent capping TiW layer during the EM stress. This phenomenon causes the enhancement of the vacancy formation and the acceleration of the line disruption. The raise of temperature during the current stress also enhances the mass flux at the junction point that resultes in the early failure of the line. Under the same current density, higher power consumption for the TiW capped line also increases the Cu diffusion rate. The resistance vs. stress time result shows that the TiW capping layer causes an increase of the line resistance leading to void formation in the bulk Cu line. Thus, the capping layer material selection is significant to the electromigration failure of the Cu line.

The objective of the TiW capping layer study is to find out whether TiW is a good capping layer for Cu lines. Also, in industry, multiply layer is very common. In order to connect Cu layer with Si dielectric material on top, the TiW capping layer on Cu is very essential.

Normally, dielectric capping layer will reduce the surface oxidation and extend the Cu lines lifetime. However, according to this study, metal may not be a good choice for the Cu lines capping layer. Even if the TiW capping layer could prevent oxidation, it causes the diffusion problem, which reduces more lifetime than oxidation. Reducing the temperature during the electromigration test is always an effective option, which could mitigate Cu diffusing into the TiW capping layer.

This research also indicates another probability that Cu lines with salient structures have longer lifetime than those with mosaic structures. Nowadays, industries use this mosaic structure Cu lines a lot. According to the TiW capping layer effect on resistance, it’s reasonable to deduct that Cu lines with mosaic structures have higher resistance and consume more power when the applied current is the same, because the Ti-Cu and W-Cu bonds still provide higher resistivity at the interface. Also, according to the diffusion theory, Cu atoms could also diffuse into the side

TiW and reduce the lifetime. The Cu reactive ion etching method used in this research can constantly etch this salient structure, which is a clear advantage of this dry etching method.

REFERENCES

1. C. C. Lin and Y. Kuo, *MRS Procs.*, **1428**, mrss12-1428-c05-03 (2012).
2. Y. Kuo and S. Lee, *Jpn. J. Appl. Phys.*, **39**(3AB), L188-L190 (2000).
3. Y. Kuo and S. Lee, *Appl. Phys. Lett.*, **78**(7), 1002-1004 (2001).
4. Y. Kuo, Proc. *16th Intl. Workshop on Active-Matrix Flat Panel Displays and Devices*, 211-214 (2009).
5. J. R. Black, *IEEE Reliability Phys. Symp.*, 142-149 (1974).
6. G. Liu and Y. Kuo, *J. Electrochem. Soc.*, **156**(7), H579-H584 (2009).
7. C. C. Lin and Y. Kuo, *J. Appl. Phys.*, **111**(6), 265 (2012).
8. O. Kraft and E. Arzt, *Acta Materialia.*, **46**(11), 3733-3743(1998).
9. E. Kinsbron, *Appl. Phys. Lett.*, **36**(12), 968-970 (1980).
10. A.V. Vairagar, S.G. Mhaisalkar, and A. Krishnamoorthy, *Microelectronics Reliability.*, **44.5**, 747-754 (2004).
11. A. Roy, R. Kumar, Tan, C.M. Wong, T. K. S. and C. Tung, *Semiconductor Sci. Technol.*, **21**(9), 1369 (2006).
12. M. C. Kang, Y. J. Kim and J. J. Kim, *Electrochemical and Solid-State Letters*, **12**(9), H340-H343 (2009).
13. Y. Kuo, *J. Electrochem. Soc.*, **137**(4), 1235 (1990).
14. T. Du, A. Vijayakumar and V. Desai, *Electrochimica Acta.*, **49**(25), 4505-4512 (2004).
15. O. Çakır, *Trans. Tech. Publications*, **364**, 460-465 (2008).
16. Y. Kuo and S. Lee, *ECS Proc.*, **99**(30), 328 (1999).
17. S. Lee and Y. Kuo, *J. Electrochem. Soc.*, **148**(9), G524-G529 (2001).
18. S. Lee and Y. Kuo, *Thin Solid Films*, (2003).

19. Y. Kuo, *Proc. ISSP*, 305-308 (2003).

20. G. Liu and Y. Kuo, *J. Electrochem. Soc.*, **155**(2), H97-H102 (2008).

21. P.A. Tamirisa, G. Levitin, N.S. Kulkarni, and D.W. Hess, *Microelectronic Engineering*, **84**, 105-108 (2007).

22. F. Wu, G. Levitin and D. W. Hess, *ACS Appl. Mater. Interfaces*, **2**(8), 2175-2179 (2010).

23. Y. Kuo, *Jpn. J. Appl. Phys*., **32**(1AB), L126-L128 (1993).

24. C. Ryu, H. Lee, K. W. Kwon, A. L. Loke and S. S. Wong, *Solid State Technology*, **42**(4), 53-56 (1999).

25. B. Gao, Y. Gao, Y. Kuo and T. Yuan, *ECST*, **85**(6), 165-170 (2018).

26. J. R. Black, *IEEE Transactions on Electron Devices*, **16**(4), 338-347 (1969).

27. J. R. Black, *Proceedings of the IEEE*, **57**(9), 1587-1594 (1969).

28. I. A. Blech, *J. Appl. Phys.*, **47**, 1203 (1976).

29. M. J. Attardo and R. Rosenberg, *J. Appl. Phys.*, **41**, 2381 (1970).

30. B. N. Agarwala, M. J. Attardo, and A. P. Ingraham, *J. Appl. Phys.*, **41**, 3954 (1970).

31. H. U. Schreiber, *Solid-State Electronics*, **28**(11), 1153-1163 (1985).

32. M. J. Attardo, R. Rutledge, and R. C. Jack, *J. Appl. Phys.*, **42**, 4343 (1971).

33. J. R. Lloyd, *Appl. Phys. Lett.*, **57**, 1167 (1990).

34. C. Kim and J. W. Morris, *J. Appl. Phys.*, **73**, 4885 (1993).

35. I. Ames, F. M. d'Heurle and R. E. Horstmann, *IBM Journal of Research and Development*, **14**(4), 461-463 (1970).

36. V. T. Srikar and C. V. Thompson, *Appl. Phys. Lett.*, **72**, 2677 (1998).

37. M. Li and Y. Kuo, *ECS. Trans.*, **86**(8), 41-47 (2018).

38. A. Buerke, H. Wendrock and K. Wetzig, *Crystal Res. Technol.*, **35**(6-7), 721-730 (2010).

39. E. Arzt, O. Kraft, R. Spolenak, *Z. Metallkunde.*, **87**, 934-942 (1996).

40. RLD. Orio, H. Ceric, J. Cervenka and S. Selberherr, *IEEE Intl. Conf. Simulation Semicond. Proc. Devs.*, 1-4 (2009).

41. L. Zhang, M. Kraatz, O. Aubel, C. Hennesthal and E. Zschechet, *Aip Conference American Institute of Physics*, **1300**(1), 3-11 (2010).

42. X. Lu, J. W. Pyun, B. Li, N. Henis, K. Neuman, K. Pfeifer and P. S. Ho, *Proceedings of the IEEE International*, 33-35 (2005).

43. J. Su, M. Li and Y.Kuo, *ECS. Trans.*, **90**(1), 65-72 (2019).

44. M. Shatzkes and J. R. Lloyd, *J. Appl. Phys.*, **59**(11), 3890-3893 (1986).

45. G. Liu, *Dissertations & Theses - Gradworks Texas A&M University ETD*, **2902** (2008).

46. A. H. Fischer, A. V. Glasow, S. Penka, and F. Ungar, *IEEE International Interconnect Technology Conference*, 139-141 (2002).

47. M. R. Sørensen, Y. Mishin and A. F. Voter, *Physical Review B*, **62**(6), 3658 (2000).

48. A. Suzuki and M. Yu, *Interface Science*, **11**(1), 131-148 (2003).

49. V. Vitek, Y. Minonishi and G.J. Wang, *J. de Physique*, **46**, 171 (1985).

50. M. Li, J. Su and Y. Kuo, *ECS. Trans.*, **89**(3), 87-92 (2019).

51. M. W. Lane, E. G. Liniger and J. R. Lloyd, *J. Appl. Phys.*, **93(**3**)**, 1417-1421 (2003).

52. J. R. Lloyd and J. J. Clement, *Thin Solid Films*, **262**, 135 (1995).

53. K. Hu, R. Rosenberg and K. L. Lee, *Appl. Phys. Lett.*, **74**, 2945 (1999).

APPENDIX A

DEPOSITION AND ETCHING CONDITION

Deposition:

Table A.1 Deposition condition

Material	TiW	Cu
Power	75 W	80 W
Gas	Ar	Ar
Flow rate	50 sccm	30 sccm
Pressure	5 mTorr	10 mTorr
Time	15 min	80 min

RIE:

Table A.2 RIE condition

Material	TiW	Cu
Power	600 W	600 W
Gas	CF_4	HCl/CF_4
Flow rate	10 sccm	20/5 sccm
Pressure	60 mTorr	70 mTorr
Time	2 min	2 min

APPENDIX B

LABVIEW TESTING PROGRAM

The input module program is built by labview, shown in Figure B.1. Figure B.1 (a) shows how the input current is calculated according to the essential input parameters. Figure B.1 (b) shows the initial setup parameters inside the program, such as initial starting voltage and voltage limit.

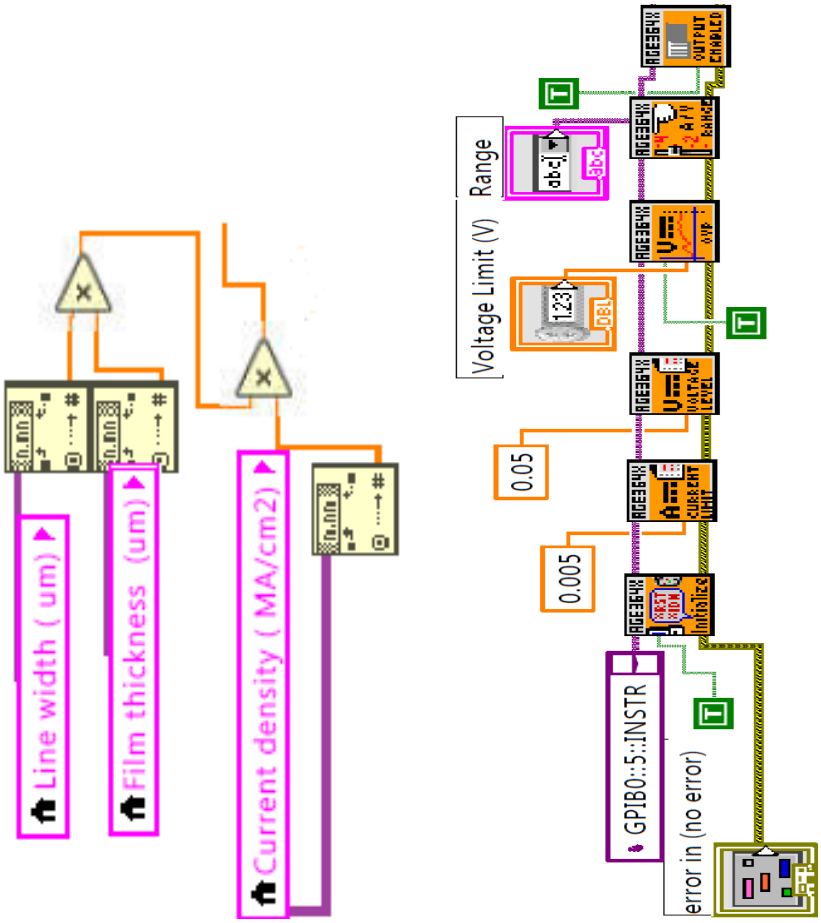

(a) (b)

Figure B.1 Input Labview program. (a) essential input parameters, (b) initial program parameter setup.

Figure B.2 shows the main algorithm of the program and the program stop trigger conditions, such as high resistance, current loss or over limit voltage.

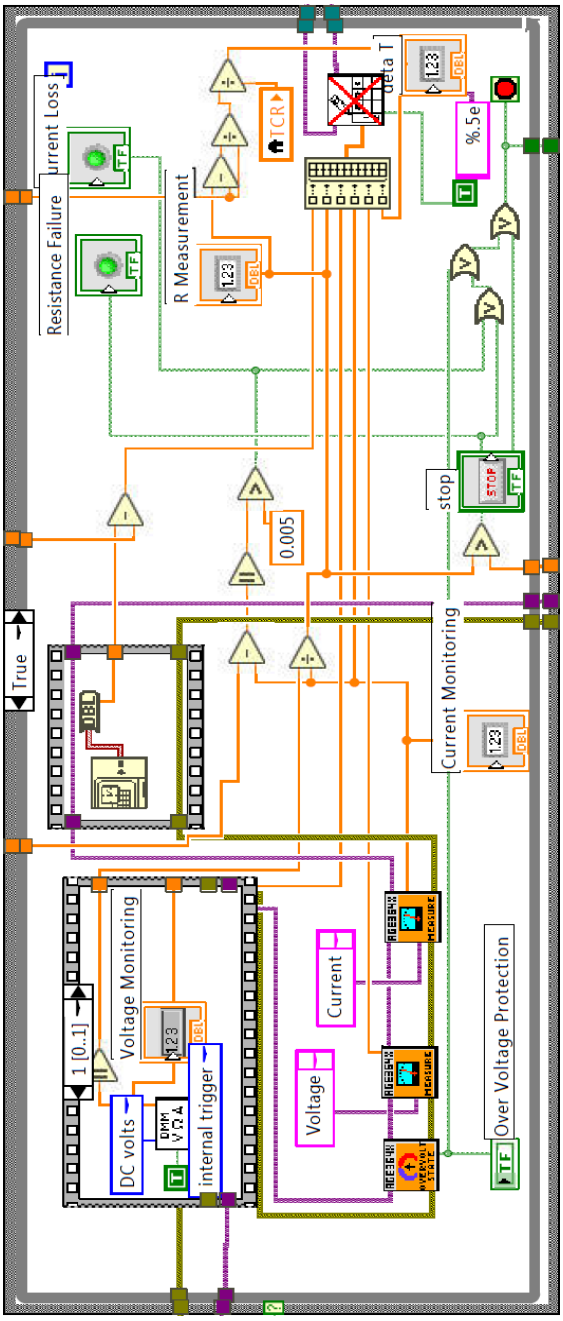

Figure B.2 Main algorithm and end program trigger module.

Figure B.3 shows how the temperature of the Cu lines is calculated during the EM test.

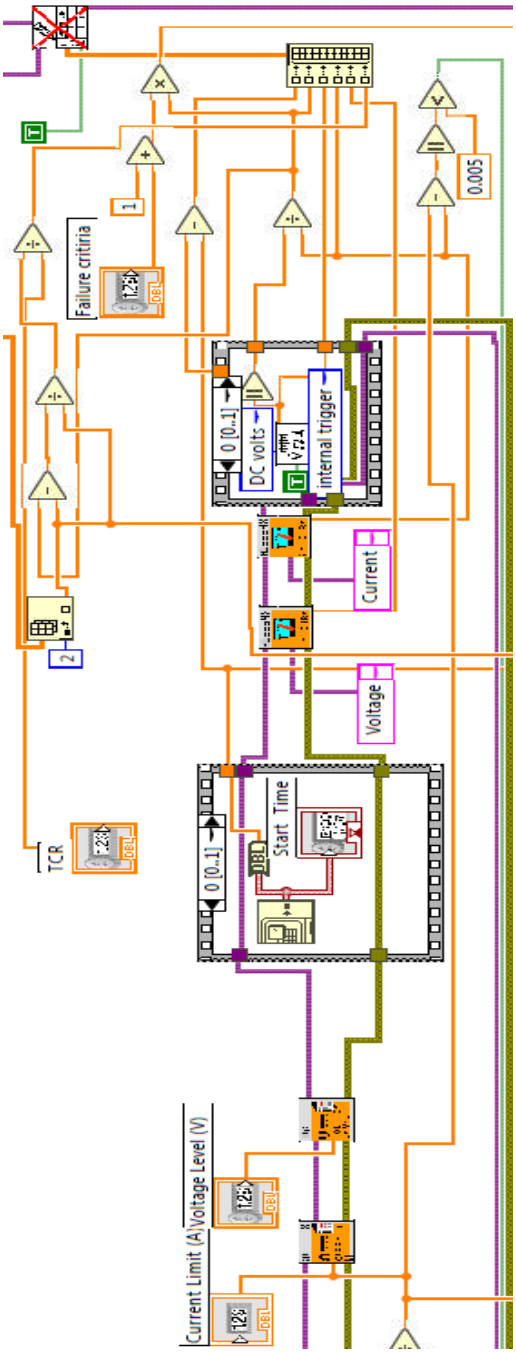

Figure B.3 Cu lines temperature calculation module.

The notification module is shown in Figure B.4. If the program ends, the system will send an email to notify the user that the system is ready for a new test.

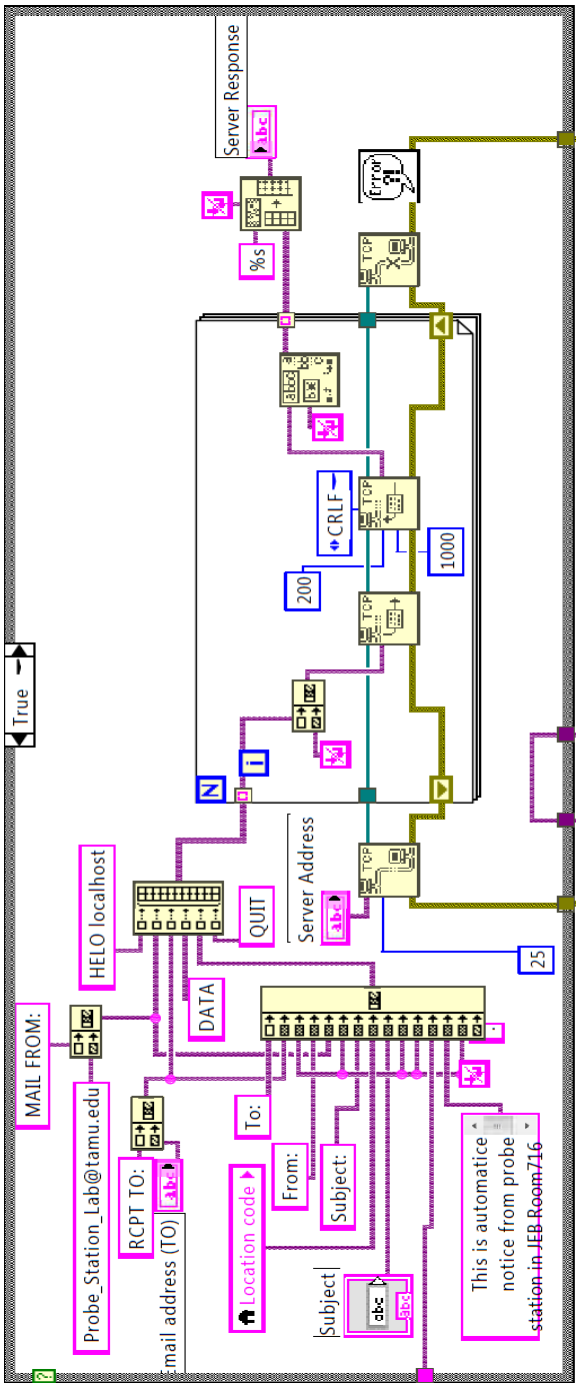

Figure B.4 System notification module.

After the program ends, system will generate a data file. The essential parameter results, shown in Figure B.5, will be included in this data file.

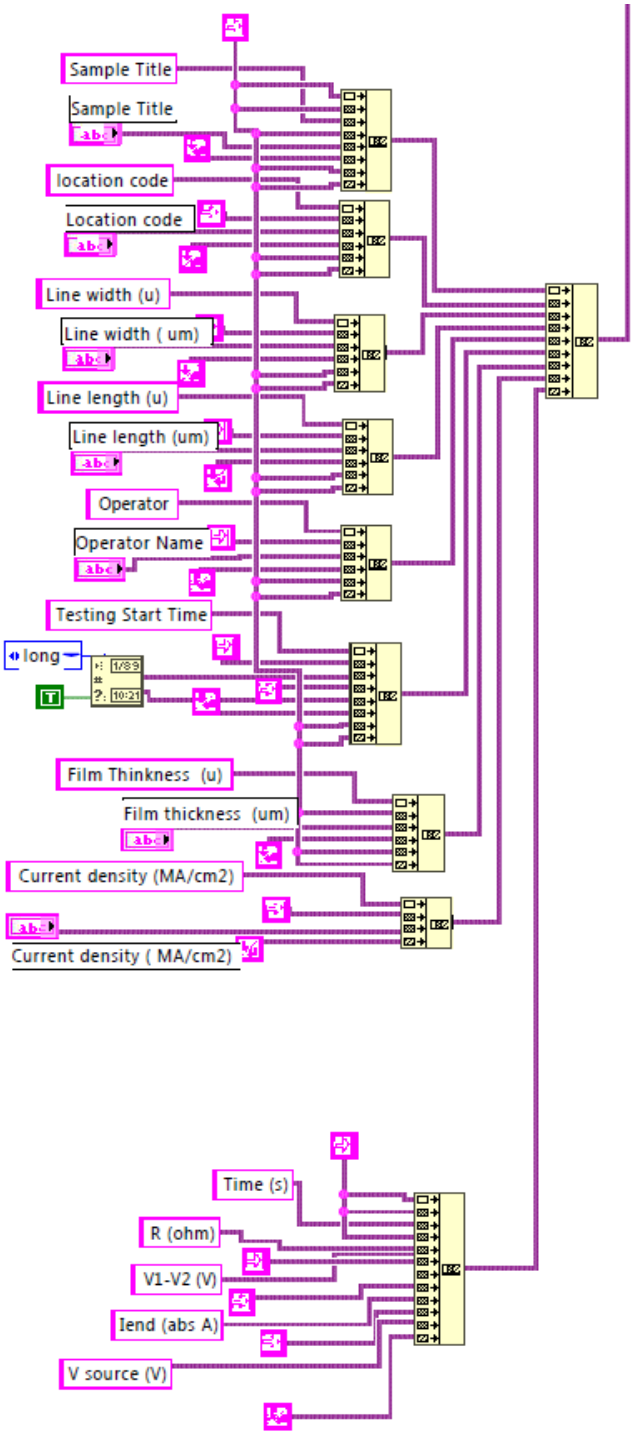

Figure B.5 Output data file module.